

EVENT-BY-EVENT PHYSICS IN RELATIVISTIC HEAVY-ION COLLISIONS

Henning Heiselberg

NORDITA, Blegdamsvej 17, DK-2100 Copenhagen Ø, Denmark

Abstract

Motivated by forthcoming experiments at RHIC and LHC, we study event-by-event fluctuations in ultrarelativistic heavy-ion collisions. Fluctuations in particle multiplicities, ratios, transverse momenta, rapidity, etc. are calculated in participant nucleon as well as thermal models. The physical observables, including multiplicity, kaon to pion ratios, and transverse momenta agree well with recent NA49 data at the SPS, and indicate that such studies do not yet reveal the presence of new physics. Predictions for RHIC and LHC energies are given. The centrality dependence with and without a phase transition to a quark-gluon plasma is discussed - in particular, how the physical quantities are expected to display a qualitative different behavior in case of a phase transition, and how a first order phase transition can be signaled by anomalous fluctuations and correlations in a number of observables.

arXiv:nucl-th/0003046v2 14 Jun 2000

Contents

1	Introduction	4
2	Phase Transitions and Fluctuations	5
2.1	Order of the QCD phase transition	6
2.2	Density, rapidity, temperature and other fluctuations	7
3	Multiplicity Fluctuations in Relativistic Heavy-Ion Collisions	9
3.1	Charged particle production in pp and $p\bar{p}$ reactions	9
3.2	Fluctuations in the participant model	13
3.3	Fluctuations in the thermal model	16
3.4	Centrality dependence and degree of thermalization	17
3.5	Enhanced fluctuations in first order phase transitions	18
4	Fluctuations and Correlations in Particle Ratios	22
4.1	K/π ratio and strangeness enhancement	22
4.2	π^+/π^- ratio and entropy production	24
4.3	π^0/π^\pm ratio and chiral symmetry restoration.	25
4.4	J/Ψ multiplicity correlations and absorption mechanisms	25
4.5	Photon fluctuations to distinguish thermal emission from $\pi^0 \rightarrow 2\gamma$	27
5	Transverse Momentum Fluctuations	28
6	Event-by-Event Fluctuations at RHIC	30
7	HBT	32
7.1	The correlation function	33
7.2	HBT for droplets	34
7.3	Centrality dependence of HBT radii	37
8	Summary	37
9	Appendix A	39

1 Introduction

The importance of event-by-event physics is evident from the following simple analogy: Stick a sheet of paper out of your window on a rainy day. Keeping it there for a long time - corresponding to averaging - the paper will become uniformly wet and one would conclude that rain is a uniform mist. If, however, one keeps the sheet of paper in the rain for a few seconds only, one observes the striking droplet structure of rain. Incidentally, one has also demonstrated the *liquid-gas phase transition!* Analysing many events gives good statistics and may reveal rare events as snow or hail and thus other phase transitions. The statistics of droplet sizes will also tell something about the fragmentation, surface tension, etc. By varying initial conditions as timing and orienting the paper, one can further determine the speed and direction of the rain drops.

Central ultrarelativistic collisions at RHIC and LHC are expected to produce at least $\sim 10^4$ particles, and thus present one with the remarkable opportunity to analyze, on an event-by-event basis, fluctuations in physical observables such as particle multiplicities, transverse momenta, correlations and ratios. Analysis of single events with large statistics can reveal very different physics than studying averages over a large statistical sample of events. The use of Hanbury Brown–Twiss correlations to extract the system geometry is a familiar application of event-by-event fluctuations in nuclear collisions [1], and elsewhere, e.g. in sonoluminescence [2]. The power of this tool has been strikingly illustrated in study of interference between Bose-Einstein condensates in trapped atomic systems [3]. Fluctuations in the microwave background radiation as recently measured by COBE [4] restrict cosmological parameters for the single Big Bang event of our Universe. Large neutron star velocities have been measured recently [5] which indicate that the supernova collapse is very asymmetrical and leads to large event-by-event fluctuations in “kick” velocities during formation of neutron stars.

Studying event-by-event fluctuations in ultrarelativistic heavy ion collisions to extract new physics was proposed in a series of papers [6–8], in which the analysis of transverse energy fluctuations in central collisions [9] was used to extract evidence within the binary collision picture for color, or cross-section, fluctuations. More recent theoretical papers have focussed on different aspects of these fluctuations, such as searching for evidence for thermalization [10–12], critical fluctuations at the QCD phase transition [13,14] and other correlations between collective quantities [15].

Results from the RHIC collider this year are eagerly awaited. The hope is to observe the phase transition to quark-gluon plasma, the chirally restored hadronic matter and/or deconfinement. This may be by distinct signals of enhanced rapidity and multiplicity fluctuations [16,13] in conjunction with J/Ψ

suppression, strangeness enhancement, η' enhancement, plateau's in temperatures, transverse flow or other collective quantities as function of centrality, transverse energy or multiplicity.

Recently NA49 has presented a prototypical event-by-event analysis of fluctuations in central Pb+Pb collisions at 158 GeV per nucleon at the SPS, which produce more than a thousand particles per event [10]. The analysis has been carried out on ~ 100.000 such events measuring fluctuations in multiplicities, particle ratios, transverse momentum, etc.

The purpose of this review is to understand these and other possible fluctuations. We find that the physical observables, including multiplicity, kaon to pion ratios, and transverse momenta agree well with recent NA49 data at the SPS, and indicate that such studies do not yet reveal the presence of new physics. Predictions for RHIC and LHC energies are given. The centrality dependence with and without a phase transition to a quark-gluon plasma is discussed - in particular, how the physical quantities are expected to display a qualitative different behavior in case of a phase transition, and how a first order phase transition can be signaled by very large fluctuations.

2 Phase Transitions and Fluctuations

Lattice QCD calculations find a strong phase transition in strongly interacting matter [17,18]. The Early Universe underwent this transition $\sim 10^{-4}$ seconds after the Big Bang and by colliding heavy nuclei we expected to reproduce this transitions at sufficiently high collisions energies.

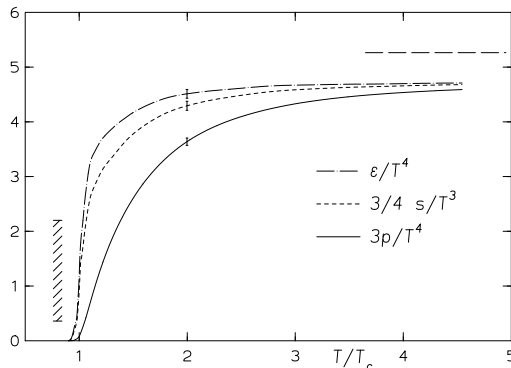


Fig. 1. Scaled energy density, entropy density and pressure vs. scaled temperature at the continuum limit in pure gauge $SU(3)$ theory [18]. The horizontal dashed line is the ideal gas limit and the vertical hatched band illustrates the latent heat.

2.1 Order of the QCD phase transition

The nature and order of the transition is not known very well. Lattice calculations can be performed for zero quark and baryon chemical potential only, $\mu_B = 0$, where they suggest that QCD has a first order transition provided that the strange quark is sufficiently light [17,18], that is for $N_f \gtrsim 3$. The transition is due to chiral symmetry restoration and occur at a critical temperature $T_C \simeq 150$ MeV. In pure SU(3) gauge theory (that is no quarks, $N_f = 0$) the transition is a deconfinement transition which also is of first order and occur at a higher temperature $T_c \simeq 260$ MeV.

However, when the strange or the up and down quark masses become heavy, the QCD transition changes to a smooth cross over. The phase diagram is then like the liquid-gas phase diagram with a critical point above which the transition goes continuously through the vapor phase. For reasonable values for the strange quark mass, $m_s \sim 150$ MeV and small up and down quark masses, the transition is, however, first order [17,18].

For exactly two massless flavors, $m_{u,d} = 0$ and $m_s = \infty$, the transition is second order at small baryon chemical potential. Random matrix theory finds a 2nd order phase transition at high temperatures which, however, change into a 1st order transition above a certain baryon density - the tricritical point.

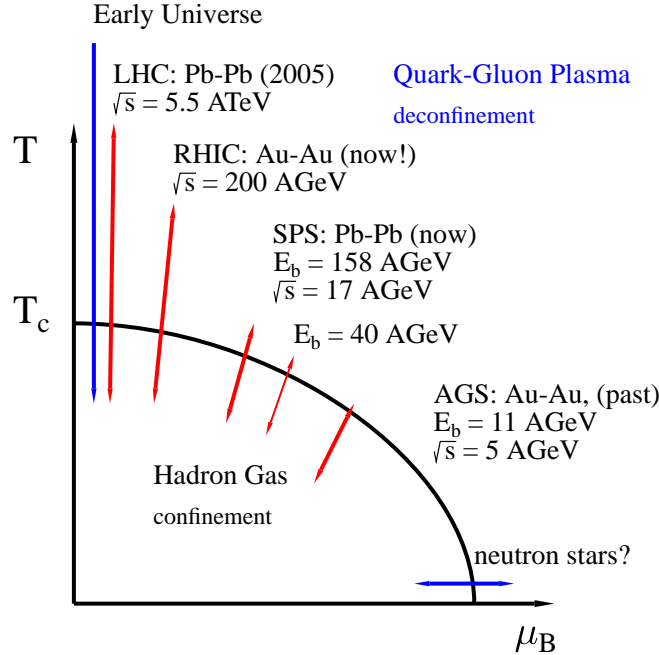


Fig. 2. An illustration of the QCD phase diagram, temperature vs. baryon chemical potential. The regions of the phase diagram probed by various high energy nuclear collisions are sketched by arrows. From [19].

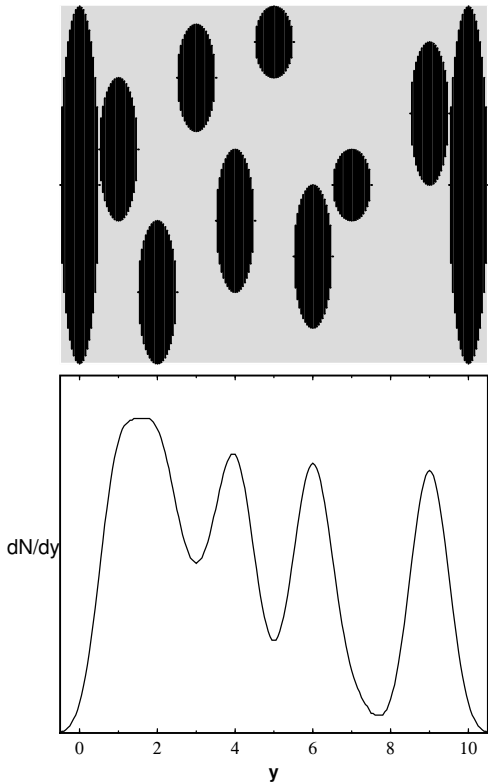


Fig. 3. Sketch of droplet formation (top) and corresponding rapidity distribution (bottom) excluding the continuous hadronic background.

2.2 Density, rapidity, temperature and other fluctuations

Fluctuations are very sensitive to the nature of the transition. In case of a second order phase transition the specific heats diverge and have been argued to reduce the fluctuations drastically [13]. For example, the temperature fluctuations have a probability distribution [20]

$$w \sim \exp(-C_V(\frac{\Delta T}{T})^2); \quad (1)$$

a diverging specific heat near a 2nd order phase transition would then remove fluctuations if matter is in global thermal equilibrium.

First order phase transition are contrarily expected to lead to large fluctuations due to droplet formation [21] or more generally density or temperature fluctuations. In case of a first order phase transition relativistic heavy ion collisions lead to interesting scenarios in which matter is compressed, heated and undergoes chiral restoration. If the subsequent expansion is sufficiently rapid, matter will pass the phase coexistence curve with little effect and supercool [22]. This suggests the possible formation of “droplets” of supercooled chiral

symmetric matter with relatively high baryon and energy densities in a background of low density broken symmetry matter. These droplets can persist until the system reaches the spinodal line and then return rapidly to the now-unique broken symmetry minimum. A large mismatch in density and energy density seems to be a robust prediction for a first order transition in random matrix theory [22].

If the transition is first order, matter may supercool and subsequently create fluctuations in a number of quantities. Density fluctuations in the form of hot spots or droplets of dense matter with hadronic gas in between is a likely outcome. We shall refer to these regions of dense and hot matter in space-time as well as in momentum space as droplets. If we assume that hadrons emerge as a Boltzmann distribution with temperature T from each droplet and ignore transverse flow, the resulting particle distribution is

$$\frac{dN}{dyd^2p_t} \propto \sum_i f_i e^{-m_t \cosh(y-\eta_i)/T}. \quad (2)$$

Here, y is the particle rapidity and p_t its transverse momentum, f_i is the number of particles hadronizing from each droplet i , and

$$\eta_i = \frac{1}{2} \log \frac{t_i + z_i}{t_i - z_i} = \frac{1}{2} \log \frac{1 + v_i}{1 - v_i} \quad (3)$$

is the rapidity of droplet i .

When $m_t/T \gg 1$, we can approximate $\cosh(y - \eta_i) \simeq 1 + \frac{1}{2}(y - \eta_i)^2$ in Eq.(2). The Boltzmann factor determines the width of the droplet rapidity distribution as $\sim \sqrt{T/m_t}$. The rapidity distribution will display fluctuations in rapidity event by event when the droplets are separated by rapidities larger than $|\eta_i - \eta_j| \gtrsim \sqrt{T/m_t}$. If they are evenly distributed by smaller rapidity differences, the resulting rapidity distribution (2) will appear flat.

The droplets are separated in rapidity by $|\eta_i - \eta_j| \sim \Delta z/\tau_0$, where Δz is the correlation length in the dense and hot mixed phase and τ_0 is the invariant time after collision at which the droplets form. Assuming that $\Delta z \sim 1\text{fm}$ — a typical hadronic scale — and that the droplets form very early $\tau_0 \lesssim 1\text{fm}/c$, we find that indeed $|\eta_i - \eta_j| \gtrsim \sqrt{T/m_t}$ even for the light pions. If strong transverse flow is present in the source, the droplets may also move in a transverse direction. In that case the distribution in p_t may be non-thermal and azimuthally asymmetric.

Even if the transition is not first order, fluctuations may still occur in the matter that undergoes a transition. The fluctuations may be in density, chiral symmetry [23], strangeness, or other quantities and show up in the associated particle multiplicities. The “anomalous” fluctuations depends not only on the

type and order of the transition, but also on the speed by which the collision zone goes through the transition, the degree of equilibrium, the subsequent hadronization process, the amount of rescatterings between hadronization and freezeout, etc. It may be that any sign of the transition is smeared out and erased before freezeout. This is the case for the event-by-event fluctuations measured at CERN [16] within experimental accuracy. Whether they remain at RHIC is yet to be discovered and we shall provide some tools for the analysis in the following sections.

3 Multiplicity Fluctuations in Relativistic Heavy-Ion Collisions

In order to be able to extract new physics associated with fluctuations, it is necessary to understand the role of expected statistical fluctuations. Our aim here is to study the sources of these fluctuations in collisions. As we shall see, the current NA49 data can be essentially understood on the basis of straightforward statistical arguments. Expected sources of fluctuations include impact parameter fluctuations, fluctuations in the number of primary collisions, and the results of such collisions, nuclear deformations [9], effects of rescattering of secondaries, and QCD color fluctuations. Since fluctuations in collisions are sensitive to the amount of rescattering of secondaries taking place, we discuss in detail two limiting cases, the participant or “wounded nucleon model” (WNM) [24], in which one assumes that particle production occurs in the individual participant nucleons and rescattering of secondaries is ignored, and the thermal limit in which scatterings bring the system into local thermal equilibrium. Whether rescatterings increase relative fluctuations through greater production of multiplicity, transverse momenta, etc., or decrease fluctuations by involving a greater number of degrees of freedom, is not immediately obvious. Indeed VENUS simulations [31] showed that rescattering had negligible effects on transverse energy fluctuations. As we shall see, both models give similar results for multiplicity fluctuations. In the wounded nucleon model fluctuations arise mainly from multiplicity fluctuations for each participant and from impact parameter fluctuations. Limited acceptance also influences the observed fluctuations. We calculate in detail statistical fluctuations in multiplicity, K/π ratios, and transverse momentum. Finally, we show in a simple model how first order phase transitions are capable of producing very significant fluctuations.

3.1 Charged particle production in pp and $p\bar{p}$ reactions

Participant models or WNM are basically a superposition of NN collisions. Such have been studied extensively at these energies within the last decades

Global Fluctuations

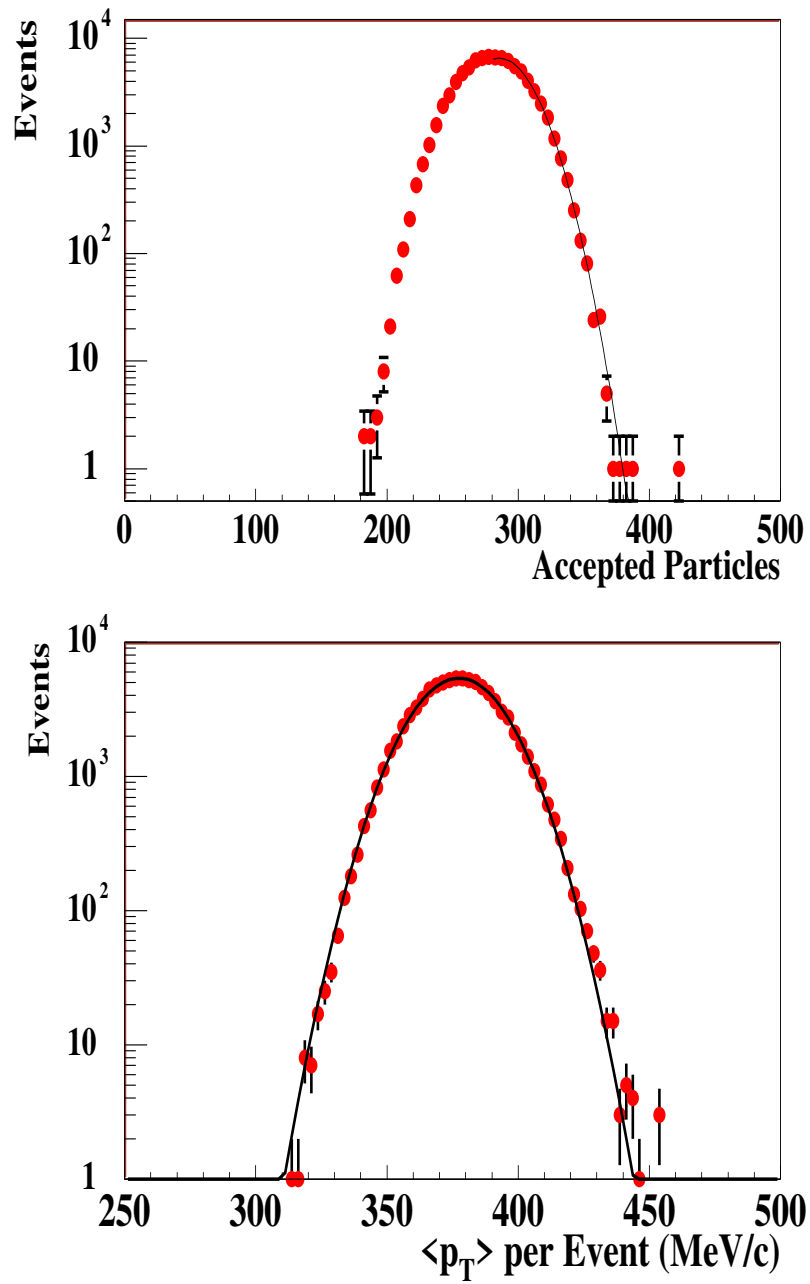


Fig. 4. Event-by-event fluctuations of multiplicity (top) and p_t (bottom) measured by NA49 in central Pb+Pb collisions at the SPS [10].

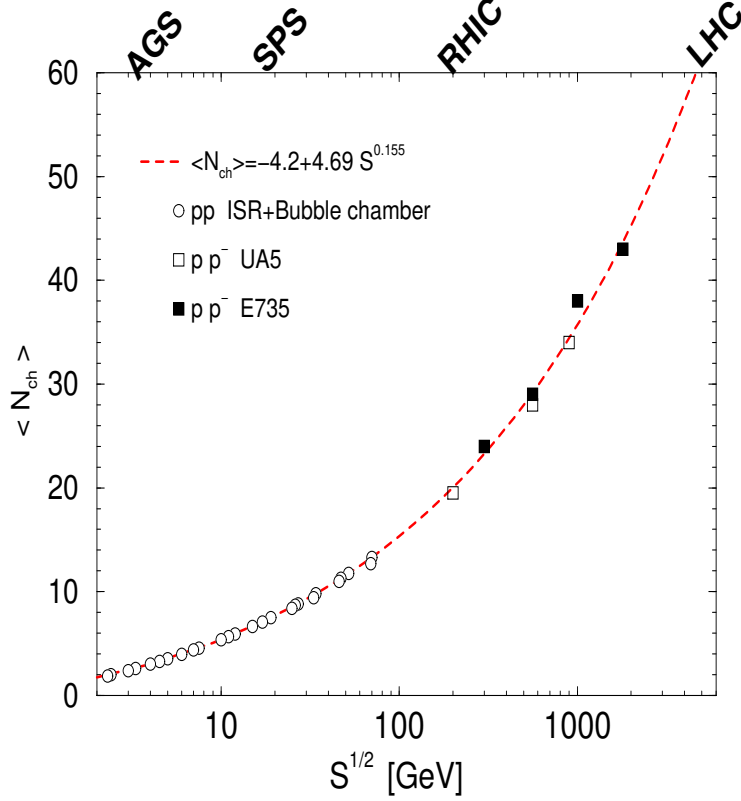


Fig. 5. The total number of charged particles produced in pp and $p\bar{p}$ collisions vs. cms energy $s^{1/2}$. Data from bubble chamber [25], ISR [26], UA5 [27] and FNAL E735 [28].

at several particle accelerators and we here give a brief compilation of relevant results.

The average number of charged particles produced in high energy pp and ultrarelativistic $p\bar{p}$ collisions can be parametrized by

$$\langle N_{ch} \rangle \simeq -4.2 + 4.69s^{0.155}, \quad (4)$$

for cms energies $\sqrt{s} \gtrsim 2$ GeV. At ultrarelativistic energies the charged particle production is very similar in pp , pn and $p\bar{p}$ collisions and the parametrization of Eq. (4) apply in a wide range of cms energies $2 \text{ GeV} \lesssim s^{1/2} \lesssim 2 \text{ TeV}$ as shown in Fig. (5). At SPS, RHIC and LHC energies, $\sqrt{s} \simeq 20, 200, 5000$ GeV, we find $\langle N_{ch} \rangle \simeq 7.3, 20, 60$, respectively.

At high energies KNO scaling [29] is a good approximation. KNO scaling imply that multiplicity distributions are invariant when scaled with the average multiplicity. Thus all moments scale like

$$\langle N_{ch}^q \rangle \simeq c_q \langle N_{ch} \rangle^q, \quad (5)$$

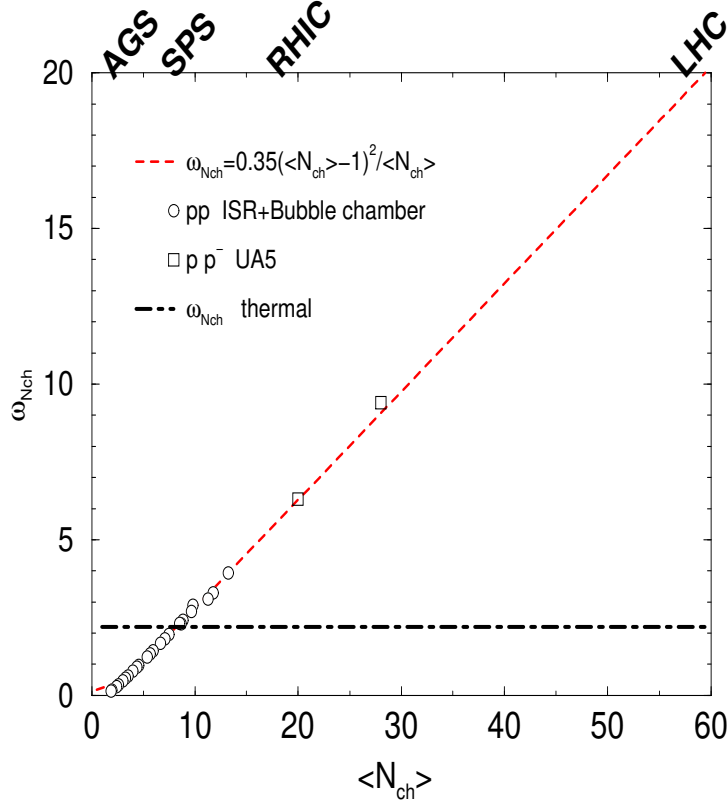


Fig. 6. The fluctuations in the total number of charged particles produced in pp and $p\bar{p}$ collisions from bubble chamber [25], ISR [26], and UA5 [27]. Note the large difference between pp and thermal fluctuations $\omega_{N_{ch}}^{th} \simeq 2.2$ at very high energies and the “accidental” crossing around SPS energies.

at high energies where c_q are constants independent of collision energy. The fluctuations, $\omega_N \equiv (\langle N^2 \rangle - \langle N \rangle^2) / \langle N \rangle$, therefore scale with average multiplicity, $\langle N \rangle$, and therefore increase with collision energy as in Eq. (4). The fluctuations in the charged particle multiplicity can be parametrized more accurately by

$$\omega_{N_{ch}} \simeq 0.35 \frac{(\langle N_{ch} \rangle - 1)^2}{\langle N_{ch} \rangle} \quad (6)$$

as shown in Fig. (6) for pp and $p\bar{p}$ collisions in the same wide range of energies. At the very high energies breakdown of KNO scaling has been observed in the direction that the fluctuations are slightly larger. At SPS, RHIC and LHC energies we find $\omega_{N_{ch}} \simeq 2.0, 6.2, 20$, respectively in pp and $p\bar{p}$ collisions.

In nuclear (AA) collisions the number of participating nucleons N_p grow with centrality and nuclear mass number A . Therefore the average charged particle multiplicity and variance grows with N_p , whereas the ratio and therefore the fluctuation $\omega_{N_{ch}}$ is independent of N_p , and equal to the fluctuations in pp collisions. (Other fluctuations such as impact parameter will be included below.)

Higher moments of the multiplicity distributions are large in high energy pp and $p\bar{p}$ collisions due to KNO scaling but in nuclear collisions such higher moments are suppressed by factors of $1/N_p$ and are therefore less interesting than the second moment. This justifies our detailed analyses of the fluctuations.

3.2 Fluctuations in the participant model

In the participant or wounded nucleon models nucleus-nucleus collisions at high energies are just a superposition of nucleon-nucleon (NN) interactions. In peripheral collisions there are only few NN collisions and the WNM should apply. For central nuclear collisions, however, multiple NN scatterings, energy degradation, rescatterings between produced particles and other effects complicate the particle production. Yet, the WNM provide a simple baseline to compare to, when going from peripheral towards central collisions.

Let us first calculate fluctuations in the participant model, which appears to describe well physics at SPS energies [10]. In this picture

$$N = \sum_i^{N_p} n_i, \quad (7)$$

where N_p is the number of participants and n_i is the number of particles produced in the acceptance by participant i . In the absence of correlations between N_p and n , the average multiplicity is $\langle N \rangle = \langle N_p \rangle \langle n \rangle$. For example, NA49 measures charged particles in the rapidity region $4 < y < 5.5$ and finds $\langle N \rangle \simeq 270$ for central Pb+Pb collisions. Finite impact parameters ($b \lesssim 3.5$ fm) as well as surface diffuseness reduce the number of participants from the total number of nucleons $2A$ to $\langle N_p \rangle \simeq 350$ estimated from Glauber theory; thus $\langle n \rangle \simeq 0.77$. Squaring Eq. (7) assuming $\langle n_i n_j \rangle = \langle n_i \rangle \langle n_j \rangle$ for $i \neq j$, we find the multiplicity fluctuations

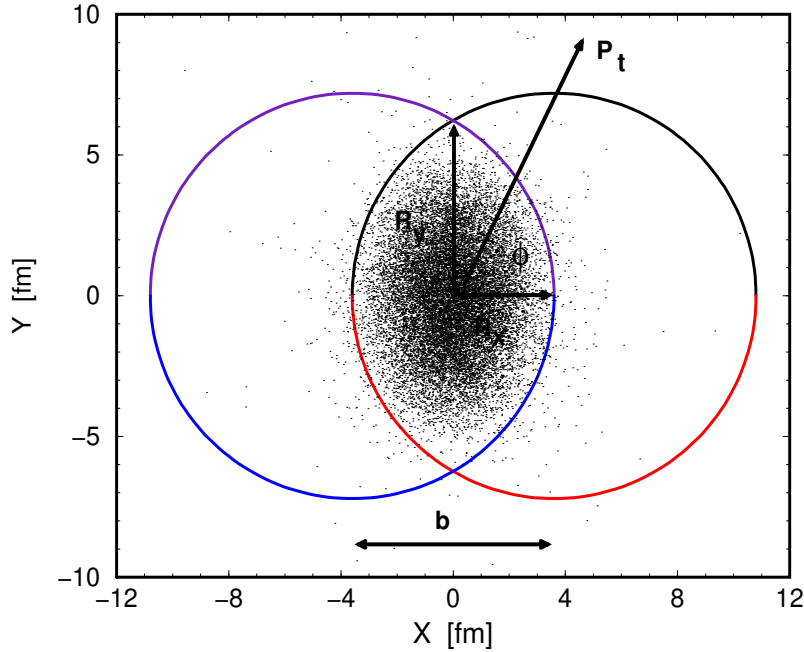
$$\omega_N = \omega_n + \langle n \rangle \omega_{N_p}, \quad (8)$$

where in general we write (see Appendix for a derivation)

$$\sigma(x) = \langle x^2 \rangle - \langle x \rangle^2 \equiv \langle x \rangle \omega_x \quad (9)$$

for any stochastic variable x .

A major source of multiplicity fluctuations per participant, ω_n , is the limited acceptance. While each participant produces ν charged particles, only a smaller fraction $f = \langle n \rangle / \langle \nu \rangle$ are accepted. Without carrying out a detailed analysis of the acceptance, one can make a simple statistical estimate assuming that the particles are accepted randomly, in which case n is binomially



□

Fig. 7. Reaction plane of semi-central $Pb + Pb$ collision for impact parameter $b = R_{Pb} \simeq 7\text{fm}$. The overlap zone is deformed with $R_x \leq R_y$. The reaction plane (x, z) is rotated by the angle ϕ with respect to the transverse particle momentum p_t which defines the outward direction in HBT analyses.

distributed with $\sigma(n) = \nu f(1 - f)$ for fixed ν . Including fluctuations in ν we obtain, similarly to Eq. (8),

$$\omega_n = 1 - f + f\omega_\nu. \quad (10)$$

In NN collisions at SPS energies, the charged particle multiplicity is ~ 7.3 and $\omega_\nu \simeq 1.9$ [32]; thus $\langle \nu \rangle \simeq 3.7$ and $f \simeq 0.21$ for the NA49 acceptance. Consequently, we find from Eq. (10) that $\omega_n \simeq 1.2$. The random acceptance assumption can be improved by correcting for known rapidity correlations in charged particle production in pp collisions [26,25].

Multiplicity generally increase with centrality of the collision. We will use the term *centrality* as impact parameter b in the collision. It is not a directly measurable quantity but is closely correlated to the transverse energy produced E_T , the measured energy in the zero degree calorimeter and the total particle multiplicity N measured in some large rapidity interval. The latter is again

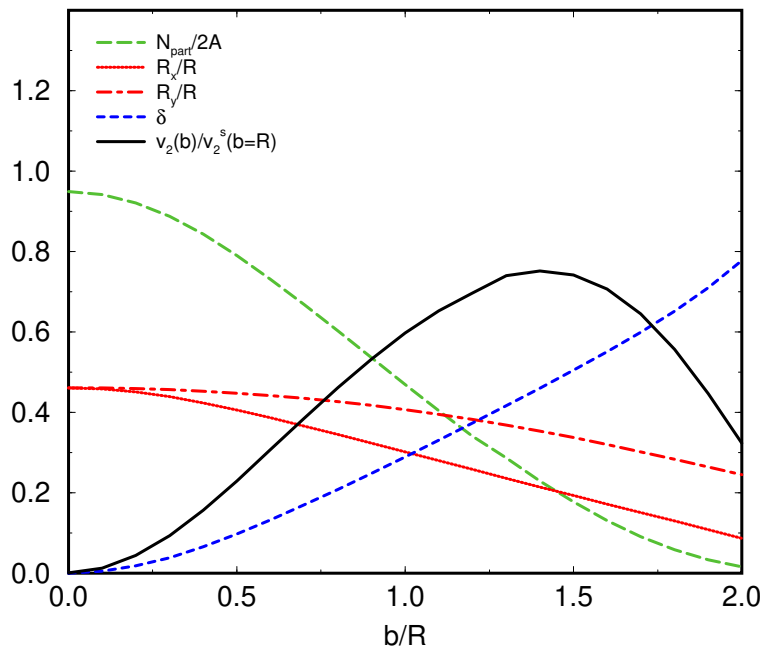


Fig. 8. Number of participants, transverse radii of nuclear overlap $R_x^2 = \langle x^2 \rangle$ and $R_y^2 = \langle y^2 \rangle$, deformation $\delta = (R_y^2 - R_x^2)/(R_y^2 + R_x^2)$, and elliptic flow parameter v_2 versus impact parameter. From [33].

approximately proportional to the number of participating nucleons

$$N_p(\mathbf{b}) = \int_{\text{overlap}} \left[\rho(\mathbf{r} + \frac{\mathbf{b}}{2}) + \rho(\mathbf{r} - \frac{\mathbf{b}}{2}) \right] d^3r. \quad (11)$$

The number of participants for colliding two spherical nuclei of radius R is shown in Fig. (8) as function of impact parameter.

As a consequence of nuclear correlations, which strongly reduce density fluctuations in the colliding nuclei, the fluctuations $\omega_{N_p(b)}$ in N_p are very small for fixed impact parameter b [8]. Almost all nucleons in the nuclear overlap volume collide and participate. [By contrast, the fluctuations in the number of binary collisions is non-negligible.] Cross section fluctuations play a small role in the WNM [8]. Fluctuations in the number of participants can arise when the target nucleus is deformed, since the orientations of the deformation axes vary from event to event [34]. The fluctuations, ω_{N_p} , in the number of participants are dominated by the varying impact parameters selected by the experiment. In the NA49 experiment, for example, the zero degree calorimeter selects the 5% most central collisions, corresponding to impact parameters smaller than

a centrality cut on impact parameter, $b_c \simeq 3.5$ fm. We have

$$\omega_{N_p} \langle N_p \rangle = \frac{1}{\pi b_c^2} \int_0^{b_c} d^2b N_p(b)^2 - \langle N_p \rangle^2, \quad (12)$$

where $\langle N_p \rangle = (1/\pi b_c^2) \int_0^{b_c} d^2b N_p(b)$. The number of participants for a given centrality, calculated in [33], can be approximated by $N_p(b) \simeq N_p(0)(1-b/2R)$ for $0 \leq b \lesssim 3.5$ fm; thus

$$\omega_{N_p} = \frac{N_p(0)}{18} \left(\frac{b_c}{2R} \right)^2. \quad (13)$$

For NA49 Pb+Pb collisions with $N_p(0) \simeq 400$ and $(b_c/2R)^2 \simeq 5\%$ we find $\omega_{N_p} \simeq 1.1$. Impact parameter fluctuations are thus important even for the centrality trigger of NA49. Varying the centrality cut or b_c to control such impact parameter fluctuations (13) should enable one to extract better any more interesting intrinsic fluctuations. Recent WA98 analyses confirm that fluctuations in photons and pions grow approximately linearly with the centrality cut [35]. The Gaussian multiplicity distribution found in central collisions changes for minimum bias to a plateau-like distribution [9].

Calculating ω_N for the NA49 parameters, we find from Eq. (8), $\omega_N \simeq 1.2 + (0.77)(1.1) = 2.0$, in good agreement with experiment, which measures a multiplicity distribution $\propto \exp[-(N - \langle N \rangle)^2/2\langle N \rangle \omega_N^{exp}]$, where ω_N^{exp} is of order 2.01 [10].

3.3 Fluctuations in the thermal model

Let us now consider, in the opposite limit of considerable rescattering, fluctuations in thermal models. In a gas in equilibrium, the mean number of particles per bosonic mode n_a is given by

$$\langle n_a \rangle = (\exp(E_a/T) - 1)^{-1}, \quad (14)$$

with fluctuations

$$\omega_{n_a} = 1 + \langle n_a \rangle. \quad (15)$$

The total fluctuation in the multiplicity, $N = \sum_a n_a$, is

$$\omega_N^{BE} = 1 + \sum_a \langle n_a \rangle^2 / \sum_a \langle n_a \rangle. \quad (16)$$

If the modes are taken to be momentum states, the resulting fluctuations are $\omega_N^{BE} = \zeta(2)/\zeta(3) = 1.37$ for massless particles, while for pions at temperature $T = 150$ MeV $\omega_N^{BE} = 1.11$ [36].

Resonances add to fluctuations in the thermal limit whereas they are implicitly included in the WNM fluctuations. In high energy nuclear collisions, resonance decays such as $\rho \rightarrow 2\pi$, $\omega \rightarrow 3\pi$, etc., lead to half or more of the pion multiplicity. Only a small fraction $r \simeq 20 - 30\%$ produce two *charged* particles in a thermal hadron gas [38] or in RQMD [37]. If not all of the decay particles fall into the NA49 acceptance the fluctuations from resonances will be reduced, $r = \text{time} \approx 0.1$. Including such resonance fluctuations in the BE fluctuations gives, similarly to Eq. (8),

$$\omega_N^{BE+R} = r \frac{1-r}{1+r} + (1+r)\omega_N^{BE}. \quad (17)$$

With $r \simeq 0.1$ we obtain $\omega_N^{BE+R} \simeq 1.3$. In [13] the estimated effect of resonances is about twice ours: $\omega_N \simeq 1.5$, not including impact parameter fluctuations.

Fluctuations in the effective collision volume add a further term $\langle N \rangle \sigma(V) / \langle V \rangle^2$ to ω_N^{BE+R} . Assuming that the volume scales with the number of participants, $\omega_V / \langle V \rangle \simeq \omega_{N_p} / \langle N_p \rangle$, we find from Eq. (8) that $\omega_N = \omega_N^{BE+R} + \langle n \rangle \omega_{N_p} \simeq 2.1$, again consistent with the NA49 data. Because of the similarity between the magnitudes of the thermal and WNM multiplicity fluctuations, the present measurements cannot distinguish between these two limiting pictures.

3.4 Centrality dependence and degree of thermalization

It is very unfortunate that the WNM and thermal models predict the same multiplicity fluctuations in the NA49 acceptance - and that they agree with the experiment. If the numbers from the two models had been different and the experimental number in between these two, then one would have had quantified the degree of thermalization in relativistic heavy ion collisions.

The similarity of the fluctuation in the thermal and WNM is, however, a coincidence at SPS energies. As seen from Fig. (6) the fluctuations in pp collisions increase with collision energy and just happen to cross the thermal fluctuations, $\omega_{\text{thermal}} \simeq 2.2$, at SPS energies.¹

At RHIC or LHC energies the situation will be much clearer. Here the charged

¹ As discussed in below the thermal fluctuations in positive or negative particles are $\omega_{\pm} \simeq 1.1$ in a thermal hadron gas. The fluctuation in total charge is twice that due to overall charge neutrality which relates the number of positive to negative particles.

particle fluctuations in pp collisions are much larger as seen in Fig. (6), namely $\omega_{N_{ch}}^{pp} = 6.5, 20$ at RHIC and LHC energies respectively. The thermal fluctuations remain at $\omega_{thermal} \simeq 2.2$. Therefore a dramatic reduction in event-by-event fluctuations are expected at higher energies at the nuclear collisions become more central.

This can be exploited to define a ‘‘Degree of thermalization’’ as the measured fluctuations at a given centrality relative to those in the thermal and pp limits

$$\text{Degree of thermalization} \simeq \frac{\omega_N^{WNM} - \omega_N^{exp}}{\omega_N^{WNM} - \omega_N^{thermal}}, \quad (18)$$

which ranges from unity in the thermal limit to zero in the WNM. Whereas both ω_N^{WNM} and ω_N^{exp} may depend on the acceptance the degree of thermalization Eq. (18) should not. Contributions from volume or impact parameter fluctuations may, however, be centrality dependent and should therefore be subtracted. Alternatively, the fluctuations in a ratio, e.g. N_-/N_+ , should be taken for limited acceptances.

The fluctuations in the number of charged particles in the NA49 acceptance is actually slightly smaller in pp collisions than thermal fluctuations. Preliminary results indicate that the fluctuations in net and total charge increase slightly going from peripheral towards central collisions [30]. Correcting for lack of full particle identification the numbers in the given acceptances seem to confirm that peripheral collisions are just a superposition of pp collisions whereas central collisions have thermal fluctuations. This indicates that the degree of thermalization does increase from zero to unity approximately linearly with centrality (specifically the energy in the zero degree calorimeter).

At RHIC and LHC it should be straight forward to measure the degree of thermalization as function of centrality. This is interesting on its own and a necessary requirement for studies of anomalous fluctuations from a phase transition.

3.5 Enhanced fluctuations in first order phase transitions

First order phase transitions can lead to rather large fluctuations in physical quantities. Thus, detection of enhanced fluctuations, beyond the elementary statistical ones considered to this point, could signal the presence of such a transition. For example, matter undergoing a transition from chirally symmetric to broken chiral symmetry could, when expanding, supercool and form droplets, resulting in large multiplicity versus rapidity fluctuations [46]. Let us imagine that N_D droplets fall into the acceptance, each producing n particles, i.e., $\langle N \rangle = \langle N_D \rangle \langle n \rangle$. The corresponding multiplicity fluctuation is (see

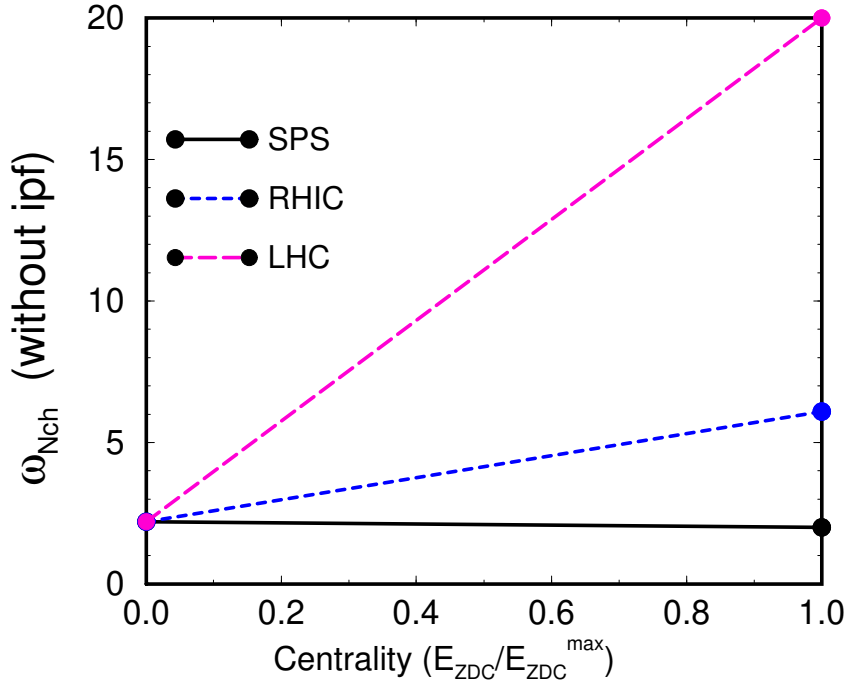


Fig. 9. The fluctuation in the total number of charged particles (excluding volume fluctuations) vs. centrality or energy in the zero degree calorimeter; left are central and right are peripheral nuclear collisions. The curves are linear extrapolations between the thermal fluctuations, $\omega_{thermal} \simeq 2.2$, in central collisions to pp fluctuations at SPS, RHIC, and LHC energies, ω^{pp} , expected in peripheral collisions within the WNM (see text).

Appendix A)

$$\omega_N = \omega_n + \langle n \rangle \omega_{N_D}. \quad (19)$$

As in Eq. (10), we expect $\omega_n \sim 1$. However, unlike the case of participant fluctuations, the second term in (19) can lead to huge multiplicity fluctuations when only a few droplets fall into the acceptance; in such a case, $\langle n \rangle$ is large and ω_{N_D} of order unity. The fluctuations from droplets depends on the total number of droplets, the spread in rapidity of particles from a droplet, $\delta y \sim \sqrt{T/m_t}$, as well as the experimental acceptance in rapidity, Δy . When $\delta y \ll \Delta y$ and the droplets are binomially distributed in rapidity, $\omega_{N_D} \simeq 1 - \Delta y/y_{tot}$, which can be a significant fraction of unity.

In the extreme case where none or only one droplet falls into the acceptance with equal probability, we have $\omega_{N_D} = 1/2$ and $\langle n \rangle = 2\langle N \rangle$. The resulting fluctuation is $\omega_N \simeq \langle N \rangle$, which is *more than two orders of magnitude larger* than the expected value of order unity as currently measured in NA49. This simple example clearly demonstrates the importance of event-by-event fluctu-

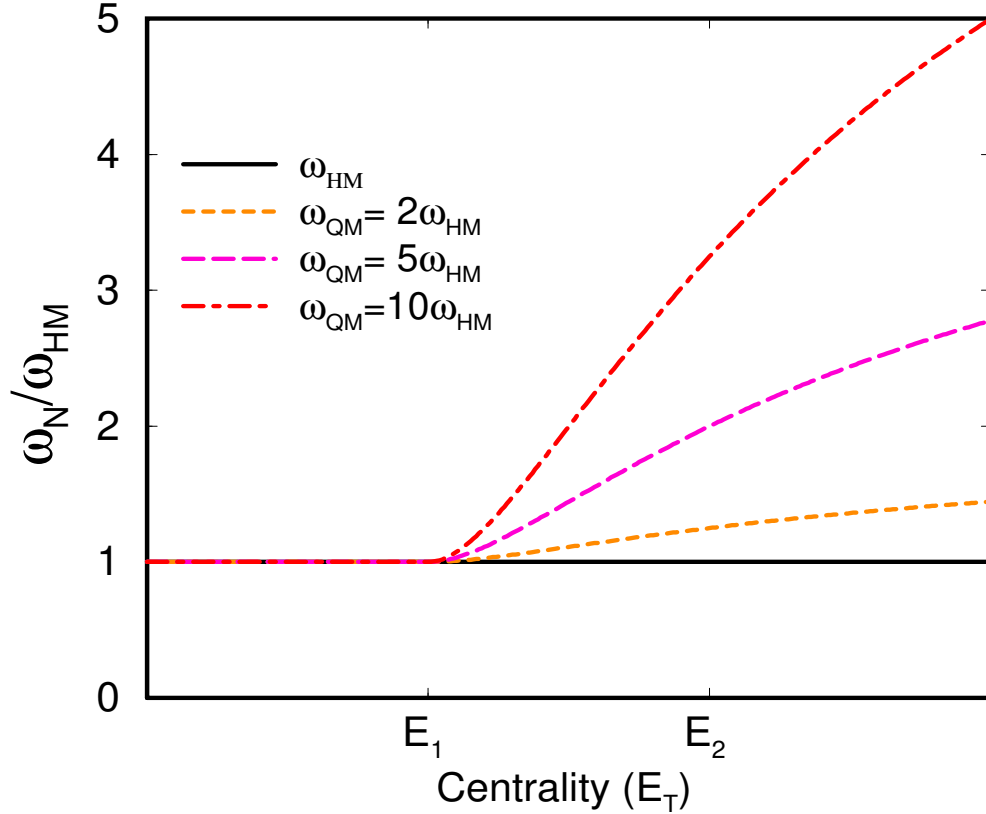


Fig. 10. Multiplicity fluctuations vs. centrality (total multiplicity or E_T). Anomalous fluctuations appear when a transition to a new state of matter (QM) starts at centrality E_1 (see text).

ations accompanying phase transitions, and illustrates how monitoring such fluctuations versus centrality becomes a promising signal, in the upcoming RHIC experiments, for the onset of a transition. The potential for large fluctuations (orders of magnitude) from a transition makes it worth looking for at RHIC considering the relative simplicity and accuracy (percents) of multiplicity measurements.

Let us subsequently consider a less extreme model in which a transition leads to enhanced fluctuations of some kind. Specifically, assume that the total multiplicity within the acceptance arise from a normal hadronic component (N_{HM}) and from a part (N_{QM}) that underwent a transition:

$$N = N_{HM} + N_{QM}; \quad (20)$$

Its average is $\langle N \rangle = \langle N_{HM} \rangle + \langle N_{QM} \rangle$. Assuming that the multiplicities from

each of the components are independent, the multiplicity fluctuation becomes

$$\omega_N = \omega_{HM} + (\omega_{QM} - \omega_{HM}) \frac{\langle N_{QM} \rangle}{\langle N \rangle}, \quad (21)$$

where $\omega_X \equiv (\langle N_X^2 \rangle - \langle N_X \rangle^2) / \langle N_X \rangle$ as earlier with $X = HM, QM$. Here, ω_{HM} is the standard fluctuation in hadronic matter $\omega_{HM} \simeq 1 - 2$, rather model independent as discussed above. The fluctuations within the component that underwent a transition, ω_{QM} depends on the type and order of the transition, the speed by which the collision zone goes through the transition, the degree of equilibrium, the subsequent hadronization process, the amount of rescatterings between hadronization and freezeout, etc. If any sign of the transition is smeared out and erased then $\omega_{QM} \simeq \omega_{HM}$, and we will not be able to see the transition in fluctuations. At the other extreme, we find the droplet scenario discussed above where $\omega_{QM} \sim \langle N \rangle \sim 10^2 - 10^3$.

The amount of QM and thus $\langle N_{QM} \rangle$ depends on centrality, energy and nuclear masses in the collision. For a given centrality the densities vary from zero at the periphery of the collision zone to a maximum value at the center. Furthermore, the more central the collision the higher energy densities are created. The transverse energy, E_T , the total multiplicity and/or the energy in the zero-degree calorimeter, E_{ZDC} , have been found to be good measures of the centrality of the collision at SPS energies. Therefore, it would be very interesting to study fluctuations vs. centrality which are proportional to energy density. By varying the binning size for centrality one can also remove impact parameter fluctuations as discussed above.

If the energy density in the center of the collision zone exceeds the critical energy density for forming QM at a certain centrality, E_1 , then a mixed phase of QM and HM is formed. At a higher energy density, where the critical energy density plus the latent heat for the transition is exceeded, which we shall assume occur at a centrality E_2 , then a pure QM phase is produced in the center. These quantities will depend on the amount of stopping at a given centrality, the geometry, T_c , etc. In the mixed phase, $E_1 \leq E_T < E_2$, the relative amount of QM, $\langle N_{QM} \rangle / \langle N \rangle$, is proportional to both the volume of the mixed phase and the fraction of the volume that is in the QM phase. The latter varies in the volume such that it vanishes at HM/QM boundary.

In Fig. (10) a schematic plot of the fluctuations of Eq. (21) is shown as function of centrality for various ω_{QM} . Up to centrality E_1 the fluctuations are unchanged. Above the central overlap zone undergoes the transition to the QM/HM mixed phase and fluctuations start to grow when $\omega_{QM} > \omega_{HM}$. At the higher centrality, E_2 the central overlap zone is in the pure QM phase but the maximum fluctuations ω_{QM} are not reached because the surface regions of the collision zone is still in the HM phase.

The multiplicity fluctuations can be studied for any kind of particles, total or ratios. Total multiplicities describe total multiplicities whereas, e.g. the ratio $\pi^0/(\pi^+ + \pi^-)$ can reveal fluctuations in chiral symmetry. The onset and magnitude of such fluctuations would reveal the symmetry and other properties of the new phase.

4 Fluctuations and Correlations in Particle Ratios

By taking ratios of particles, e.g. K/π , π^+/π^- , π^0/π^\pm , ..., one removes volume and impact parameter fluctuations to first approximation. Simply increasing/decreasing the volume or centrality, the average number of particles of both species scales up/down by the same amount and thus cancel in the ratio.

Fluctuations in various particles can reveal very different physics as will be demonstrated in the following.

4.1 K/π ratio and strangeness enhancement

To second order in the fluctuations of the numbers of K and π , we have

$$\langle K/\pi \rangle = \frac{\langle K \rangle}{\langle \pi \rangle} \left(1 + \frac{\omega_\pi}{\langle \pi \rangle} - \frac{\langle K\pi \rangle - \langle K \rangle \langle \pi \rangle}{\langle K \rangle \langle \pi \rangle} \right). \quad (22)$$

The corresponding fluctuations in $\langle K/\pi \rangle$ are given by

$$D^2 \equiv \frac{\omega_{K/\pi}}{\langle K/\pi \rangle} = \frac{\omega_K}{\langle K \rangle} + \frac{\omega_\pi}{\langle \pi \rangle} - 2 \frac{\langle K\pi \rangle - \langle K \rangle \langle \pi \rangle}{\langle K \rangle \langle \pi \rangle}. \quad (23)$$

The fluctuations in the kaon to pion ratio is dominated by the fluctuations in the number of kaons alone. The third term in Eq. (23) includes correlations between the number of pions and kaons. It contains a negative part from volume fluctuations, which removes the volume fluctuations in ω_K and ω_π since such fluctuations cancel in any ratio. In the NA49 data [10] the average ratio of charged kaons to charged pions is $\langle K/\pi \rangle = 0.18$ and $\langle \pi \rangle \simeq 200$. Excluding volume fluctuations, we take $\omega_K \simeq \omega_\pi \simeq 1.2 - 1.3$ as discussed above. The first two terms in Eq. (23) then yield $D \simeq 0.20 - 0.21$ in good agreement with preliminary measurements $D = 0.23$ [10]. Thus at this stage the data gives no evidence for correlated production of K and π , as described by the final term in Eq. (23), besides volume fluctuations. The similar fluctuations in mixed event analyses $D_{mixed} = 0.208$ [10] confirm this conclusion.

Strangeness enhancement has been observed in relativistic nuclear collisions

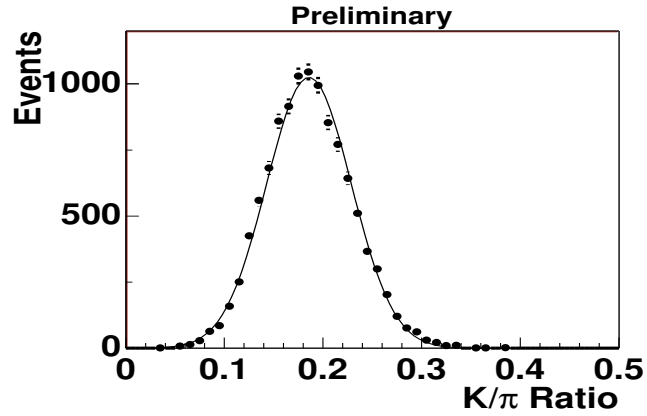


Fig. 11. Event-by-event fluctuations in the K/π ratio measured by NA49 in central Pb+Pb collisions at the SPS [10].

at the SPS. For example, the number of kaons and therefore also $\langle K/\pi \rangle$ is increased by a factor of 2-3 in central Pb+Pb collisions. It would be interesting to study the fluctuations in strangeness as well. By varying the acceptance one might be able to gauge the degree of thermalization as discussed above. The fluctuations in the K/π ratio as function of centrality would in that case reveal whether strangeness enhancement is associated with thermalization or

other mechanisms lie behind. In a plasma of deconfined quarks strangeness is increased rapidly by $q\bar{q} \rightarrow s\bar{s}$ processes and lead to enhancement of average strangeness as well as fluctuations in case of density fluctuations or droplet formation at very early times around chemical freezeout. Such strangeness fluctuations would survive even if the density fluctuations are erased during hadronization and thermal freezeout.

4.2 π^+/π^- ratio and entropy production

The fluctuations in the π^+/π^- ratio have been studied in detail in [38]. They find that resonances such as ρ, ω, \dots decaying into two or three pions tend to correlate the π^+ and π^- production. Consequently, the fluctuation in the π^+/π^- ratio is reduced by $\sim 30\%$ in good agreement with NA49 data. In turn the reduced fluctuations can be exploited to reveal the precise amount of resonances decaying into charged pions, kaons, etc.

If a quark-gluon plasma is produced it may have interesting effects on the fluctuations in the π^+/π^- ratio. The particle or entropy density of quarks, anti-quarks and gluons is a factor ~ 5 larger than for a hadron gas at $T_c \simeq 150$ MeV. An increased entropy density in the collisions volume will therefore lead to enhanced multiplicity as compared to a standard hadronic scenario if total entropy is conserved. The associated particle production must conserve net charge on large rapidity scales ($\Delta y \gtrsim 1$) due to causality because fields cannot communicate over large distances and therefore must conserve charge within the “event horizon”. Therefore the net charge, $N_+ - N_-$, is approximately conserved whereas the total charge, $N_+ + N_-$, increase by an amount proportional to the additional entropy produced. The fluctuations ω_{π^+/π^-} and the dispersion D_{\pm}^2 of Eq. (23) in the π^+/π^- ratio are both proportional to the charge difference squared divided by the total charge to the first and second power respectively. The dispersion of Eq. (23) is therefore

$$D_{\pm}^2 = \frac{\omega_{\pi^+/\pi^-}}{\langle \pi^+/\pi^- \rangle} = D_{\pm, HM}^2 \left(\frac{\langle N_{HM} \rangle}{\langle N \rangle} \right)^2, \quad (24)$$

where $D_{\pm, HM}^2$ is the dispersion in standard hadronic matter [38]. The dispersion decrease with the square of the increased total multiplicity $\langle N \rangle$ with respect to the multiplicity in a hadronic scenario $\langle N_{HM} \rangle$, which can be estimated in the WNM.

As an example, assume that the entropy density, and therefore also the multiplicity, increase from a hot hadronic gas to a quark-gluon plasma by a factor ~ 5 and approximately half of the volume is involved in this transition. The dispersion is then according to Eq. (24) suppressed by a factor $\sim 5^2/2$, i.e.

about an order of magnitude.

At SPS energies the total particle multiplicity is only slightly larger than that predicted from participant nucleon models (WNM) based on multiplicities from individual NN collisions. Therefore there is little additional entropy production, i.e., $\langle N \rangle \simeq \langle N_{HM} \rangle$ and consequently it is no surprise that the fluctuation in π^+/π^- can be explained by standard hadronic fluctuations corrected for resonances [38].

The restriction of vanishing net charge production over large rapidity scales may only be partly fulfilled and certainly in small rapidity intervals, $\Delta y \lesssim 1$, it breaks down and fluctuations should increase towards that in standard hadronic matter. Consequently, the fluctuations in π^+/π^- should depend sensitively on the rapidity interval Δy .

Again, it is important to monitor the fluctuations and dispersion D_{\pm}^2 as function of centrality. An anomalous suppression starting at some centrality would be a signal of additional entropy and particle production from, e.g., a phase transition.

4.3 π^0/π^{\pm} ratio and chiral symmetry restoration.

Fluctuations in neutral relative to charged pions would be a characteristic signal of chiral symmetry restoration in heavy ion collisions. If, during expansion and cooling, domains of chiral condensates gets “disoriented” (DCC), anomalous fluctuations in π^0/π^{\pm} ratios could result if DCC domains are large. For single DCC domain the probability distribution of ratios $d = \pi^0/(\pi^0 + \pi^+ + \pi^-)$ is $P(d) = 1/\sqrt{2d}$ with mean $\langle d \rangle = 1/3$ and fluctuation $\omega_d = 4/15$, i.e. much larger than ordinary fluctuations in such ratios (see Eq. (23)) which decrease inversely with the number of pions.

Neutral pions are much harder to measure than charged pions but with respect to fluctuations, it does not matter! The anomalous fluctuations in π^0 due to a DCC are anti-correlated to π^{\pm} , i.e. they are of same magnitude but opposite sign.

4.4 J/Ψ multiplicity correlations and absorption mechanisms

J/Ψ suppression has been found in relativistic nuclear collisions [39] and it is yet unclear how much is due to absorption on participant nucleons and produced particles (comovers). Whether “anomalous suppression” is present in the data is one of the most discussed signals from a hot and dense phase at

early times [39]. It was originally suggested that the formation of a quark-gluon plasma would destroy the $c\bar{c}$ bound states [40].

In relativistic heavy ion collisions very few J/Ψ 's are produced in each collision. Of these only 6.9% branch into dimuons that can be detected and so the chance to detect two dimuon pair in the same event is very small. Therefore, it will be correspondingly difficult to measure fluctuations and other higher moments of the number of J/Ψ .

Another more promising observable is the correlations between the multiplicities in, e.g., a rapidity interval Δy of a charmonium state $\psi = J/\Psi, \psi', \dots$ (N_ψ) and all particles (N). The correlator: $\langle NN_\psi \rangle - \langle N \rangle \langle N_\psi \rangle$ also enters the in the ratio ψ/N (see Eq. (22)). The correlator has as good statistics as the total number of ψ and it may contain some very interesting anti-correlations, namely that ψ absorption grow with multiplicity N . The physics behind can be comover absorption, which grows with comover density, or formation of quark-gluon plasma, which may lead to both anomalous suppression of ψ and large multiplicity in Δy . Contrarily, direct Glauber absorption should not depend on the multiplicity of produced particles N since it is caused by collisions with participating nucleons.

To quantify this anti-correlation we model the absorption/destruction of ψ 's by simple Glauber theory

$$\frac{N_\psi}{N_\psi^0} = e^{-\langle \sigma_{c\psi} \rho_{cl} \rangle} \equiv e^{-\gamma N / \langle N \rangle}, \quad (25)$$

where N_ψ^0 is the number of J/Ψ 's before comover or anomalous absorption sets in but after direct Glauber absorption on participant nucleons. In Glauber theory the exponent is the absorption cross section times the absorber density and path length traversed in matter. The density and therefore also the exponent is proportional to the multiplicity N with coefficient

$$\gamma = - \frac{d \log N_\psi}{d \log N} \Big|_{N=\langle N \rangle}. \quad (26)$$

In a simple comover absorption model for a system with longitudinal Bjorken scaling, it can be calculated approximately [41]

$$\gamma \simeq \sum_c \frac{dN_c}{dy} \frac{\langle v_{c\psi} \sigma_{c\psi} \rangle}{4\pi R^2} \log R / \tau_0, \quad (27)$$

where dN_c/dy , $\sigma_{c\psi}$, $v_{c\psi}$ and τ_0 are the comover rapidity density, absorption cross section, relative velocity and formation time respectively.

On average comover or anomalous absorption is responsible for a suppression

factor $e^{-\gamma}$. It is difficult to determine because only the total ψ suppression including direct Glauber absorption on participants is measured.

The anti-correlation is straight forward to calculate when the fluctuations in the exponent are small (i.e. $\gamma\sqrt{\omega_N/\langle N \rangle} \ll 1$). It is

$$\langle NN_\psi \rangle - \langle N \rangle \langle N_\psi \rangle = -\gamma\omega_N \langle N_\psi \rangle. \quad (28)$$

It is negative and proportional to the amount of comover and anomalous absorption and obviously vanishes when the absorption is independent on multiplicity ($\gamma = 0$). The anti-correlation can be accurately determined as the current accuracy in determining $\langle N_\psi \rangle$ is a few percent (NA50 minimum bias [39]) in each E_T bin.

The anti-correlations in Eq. (28) may seem independent of the rapidity interval. However, it should not be less than the typical relative rapidities between comovers and the ψ or rapidity range of the droplet.

The anticorrelations of Eq. (28) quantifies the amount of comover or anomalous absorption and can therefore be exploited to distinguish between these and direct Glauber absorption mechanisms. In that respect it is similar to the elliptic flow parameter for ψ [41] for the comover absorption part but differs for the anomalous absorption.

4.5 Photon fluctuations to distinguish thermal emission from $\pi^0 \rightarrow 2\gamma$

WA98 have measured photon and charged particle multiplicities and their fluctuations versus centrality and E_T binning size. As mentioned above impact parameter fluctuations are proportional to the E_T binning size and the WA98 analysis nicely confirms this, and can subsequently remove impact parameter fluctuations. The resulting charged particle multiplicity fluctuations with impact parameter fluctuations subtracted, $\omega_N - \langle n \rangle \omega_{N_p} \simeq 1.1 - 1.2$ were shown in Fig. (9).

The fluctuations in photon multiplicities were found to be almost twice as large as for charged particles $\omega_\gamma - \langle n \rangle \omega_{N_p} \simeq 2.0$. This has the simple explanation that photons mainly are produced in $\pi^0 \rightarrow 2\gamma$ decays. The fluctuations are then the *double* of the fluctuations in π^0 to first approximation as seen from Eq. (17).

If the photons were produced from a thermal fireball one would expect that they would exhibit Bose-Einstein fluctuations, $\omega_\gamma = \omega_N^{BE} = 1.37$ for massless particles. Photon fluctuations can therefore be exploited to quantify the amount of thermal emission vs. $\pi^0 \rightarrow 2\gamma$ decay from a hadronic gas.

5 Transverse Momentum Fluctuations

The total transverse momentum per event

$$P_t = \sum_{i=1}^N p_{t,i}, \quad (29)$$

is very similar to the transverse energy, for which fluctuations have been studied extensively [9,7]. The mean transverse momentum and inverse slopes of distributions generally increase with centrality or multiplicity. Assuming that $\alpha \equiv d \log(\langle p_t \rangle_N) / d \log N$ is small, as is the case for pions [42], the average transverse momentum per particle for given multiplicity N is to leading order

$$\langle p_t \rangle_N = \langle p_t \rangle (1 + \alpha(N - \langle N \rangle) / \langle N \rangle). \quad (30)$$

where $\langle p_t \rangle$ is the average over all events of the single particle transverse momentum. With this parametrization, the average total transverse momentum per particle in an event obeys $\langle P_t / N \rangle = \langle p_t \rangle$. When the transverse momentum is approximately exponentially distributed with inverse slope T in a given event, $\langle p_{t,i} \rangle = 2T$, and $\sigma(p_{t,i}) = 2T^2 = \langle p_t \rangle^2 / 2$. This latter fluctuation is in principle dependent on multiplicity, but as a higher order effect, we ignore it in the following.

The total transverse momentum per particle in an event has fluctuations

$$\langle N \rangle \sigma(P_t / N) = \sigma(p_t) + \alpha^2 \langle p_t \rangle^2 \omega_N + \left\langle \frac{1}{N} \sum_{i \neq j} (p_{t,i} p_{t,j} - \langle p_t \rangle^2) \right\rangle. \quad (31)$$

The three terms on the right are respectively:

i) The individual fluctuations $\sigma(p_{t,i}) = \langle p_{t,i}^2 \rangle - \langle p_t \rangle^2$, the main term. In the NA49 data, $\langle p_t \rangle = 377$ MeV and $\langle N \rangle = 270$. From Eq. (31) we thus obtain $(\sigma(P_t / N))^{1/2} / \langle p_t \rangle \simeq 1 / \sqrt{2 \langle N \rangle} = 4.3\%$, which accounts for most of the experimentally measured fluctuation 4.65% [10]. The data contains no indication of intrinsic temperature fluctuations in the collisions.

ii) Effects of correlations between p_t and N , which are suppressed with respect to the first term by a factor $\sim \alpha^2$. In NA49 the multiplicity of charged particles is mainly that of pions for which $T \simeq \langle p_t \rangle / 2$ increases little compared with pp collisions, and $\alpha \simeq 0.05 - 0.1$. Thus, these correlations are small for the NA49 data. However, for kaons and protons, α can be an order of magnitude larger as their distributions are strongly affected by the flow observed in central collisions [42].

iii) Correlations between transverse momenta of different particles in the same

event. In the WNM the momenta of particles originating from the same participant are correlated. In Lund string fragmentation, for example, a quark-antiquark pair is produced with the same p_t but in opposite direction. The average number of pairs of hadrons from the same participant is $\langle n(n-1) \rangle$ and therefore the latter term in Eq. (31) becomes $(\langle n(n-1) \rangle \langle n \rangle) (\langle p_{t,i} p_{t,j \neq i} \rangle - \langle p_t \rangle^2)$. To a good approximation, n is Poisson distributed, i.e., $\langle n(n-1) \rangle / \langle n \rangle = \langle n \rangle$, equal to 0.77 for the NA49 acceptance, so that this latter term becomes $\simeq (\langle p_{t,i} p_{t,j \neq i} \rangle - \langle p_t \rangle^2)$. The momentum correlation between two particles from the same participant is expected to be a small fraction of $\sigma(p_{t,i})$.

To quantify the effect of rescatterings, Ref. [11] suggested studying the differences in $\langle N \rangle \sigma(P_t/N)$ and $\sigma(p_t)$ via the quantity

$$\Phi(p_t) \simeq \sqrt{\langle N \rangle \sigma(P_t/N)} - \sqrt{\sigma(p_{t,i})}. \quad (32)$$

As we see from Eq. (31), in the applicable limit that the second and third terms are small,

$$\Phi(p_t) \simeq \frac{1}{\sqrt{\sigma(p_{t,i})}} \left(\alpha^2 \langle p_t \rangle^2 \omega_N + (\langle p_{t,i} p_{t,j \neq i} \rangle - \langle p_t \rangle^2) \right). \quad (33)$$

In the Fritiof model, based on the WNM with no rescatterings between secondaries, one finds $\Phi(p_t) \simeq 4.5$ MeV. In the thermal limit the correlations in Eq. (32) should vanish for classical particles but the interference of identical particles (HBT correlations) contribute to these correlations by ~ 6.5 MeV [12] and slightly reduced by resonances. The NA49 experimental value, $\Phi(p_t) = 5$ MeV (corrected for two-track resolution) seems to favor the thermal limit [10]. Note however that with $\alpha \simeq 0.05 - 0.1$, the second term on the right side of Eq. (33) alone leads to $\Phi \simeq 1 - 4$ MeV, i.e., the same order of magnitude. If $(\langle p_{t,i} p_{t,j \neq i} \rangle - \langle p_t \rangle^2)$ is not positive, then one cannot a priori rule out that the smallness of $\Phi(p_t)$ does not arise from a cancellation of this term with $\alpha^2 \langle p_t \rangle^2 \omega_N$, rather than from thermalization.

The covariance matrix between multiplicity and transverse momentum has been analysed by NA49 [43]. Strong but trivial correlations is found due to the fact that higher multiplicity gives larger total transverse momentum event-by-event. This correlation is removed in the quantity P_t/N and its covariance matrix with multiplicity appear diagonal.

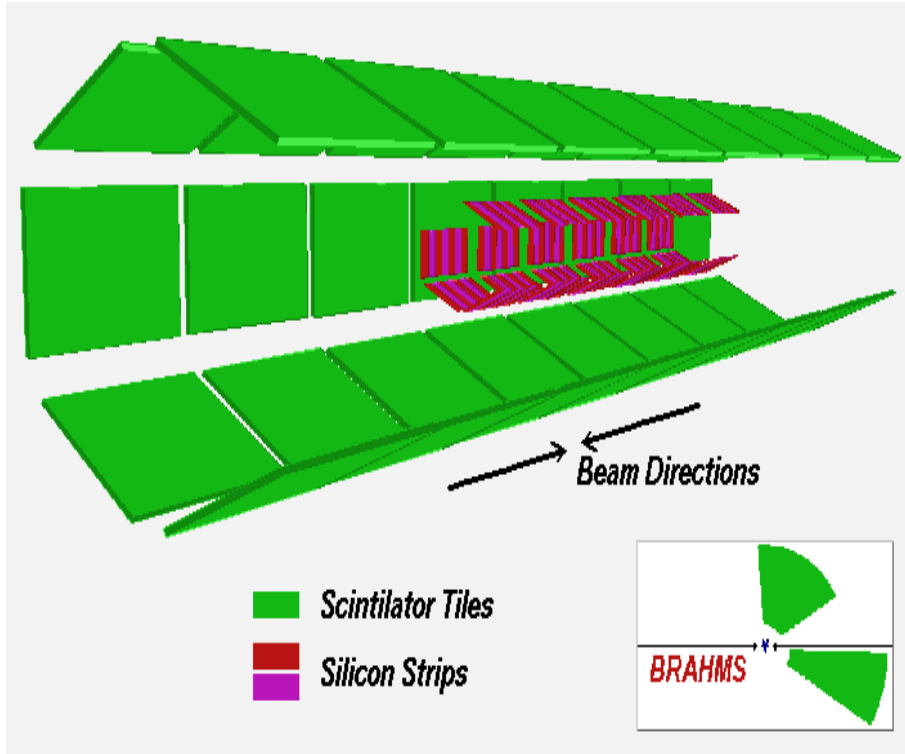


Fig. 12. Layout of the central multiplicity detector array in the BRAHMS experiment consisting of 36 scintillator tiles and 24 silicon wafers. The high resolution but slow wafers are each segmented into 7 strips giving 42 pseudo-rapidity bins along the beamline in the midrapidity interval $-2.5 \leq \eta \leq 2.5$. The fast scintillators are used as triggers for central events. The detectors surround the beamline hexagonally on 5 sides with the sixth kept open for the central spectrometer (TPC).

6 Event-by-Event Fluctuations at RHIC

The theoretical analysis above leads to a qualitative understanding of event-by-event fluctuations and speculations on how phase transitions may show up. It gives a quantitative description of AGS and SPS data without the need to invoke new physics. We shall here look ahead at RHIC experiments and attempt to describe how fluctuations may be searched for. Specifically, we shall tailor our analysis to the BRAHMS (Broad RAnge Hadron Magnetic Spectrometers) experiments as seen in Fig. (12).

Let us specifically study the energy, E_i , deposited in detector i in a given event. The total energy deposited in the event is

$$E_{Tot} = \sum_i^D E_i, \quad (34)$$

and can be used as a measure of the centrality of the collision. The energy deposited in each element (or group of elements) is the sum over the number

of particle tracks (N_i) hitting detector i of the individual ionization energy of each particle (ϵ_i)

$$E_i = \sum_n^{N_i} \epsilon_n. \quad (35)$$

The average is: $\langle E_i \rangle = \langle N_i \rangle \langle \epsilon \rangle$. The energy will approximately be gaussian distributed, $d\sigma/dE_i \propto \exp(-(E_i - \langle E_i \rangle)^2/2\omega_{E_i}\langle E_i \rangle)$, with fluctuations (see Appendix A)

$$\omega_{E_i} \equiv \frac{\langle E_i^2 \rangle - \langle E_i \rangle^2}{\langle E_i \rangle} = \omega_\epsilon + \langle \epsilon \rangle \omega_{N_i}. \quad (36)$$

Here, the fluctuation in ionization energy per particle

$$\frac{\omega_\epsilon}{\langle \epsilon \rangle} = \frac{\langle \epsilon^2 \rangle}{\langle \epsilon \rangle^2} - 1, \quad (37)$$

depends on the typical particle energies in the detector and the corresponding ionization energies for the detector type and thickness. For the BRAHMS detectors we estimate $\omega_\epsilon/\langle \epsilon \rangle \simeq 0.25$ [44]. As these are “trivial” detector parameter, we shall exclude the fluctuations ω_ϵ in the following analysis and concentrate on the second term in Eq. (36) which is the fluctuations in the number of particles as was examined in detail above.

More generally we define the multiplicity correlations between two bins also referred to as the covariance

$$\omega_{ij} = \frac{\langle N_i N_j \rangle - \langle N_i \rangle \langle N_j \rangle}{\sqrt{\langle N_i \rangle \langle N_j \rangle}} \quad (38)$$

When i, j refer to two rapidity bins the covariance is also proportional to the rapidity (auto-)correlation function $C(y_i - y_j)$.

It is instructive to consider first the complete random (uncorrelated or statistical) particle emission. For a fixed total multiplicity N_{Tot} , the probability for a particle to end up in bin i is $p_i = \langle N_i \rangle / N_{Tot} \simeq \langle E_i \rangle / E_{Tot}$. The distribution is a simple multinomial distribution for which

$$\omega_{ij} = \begin{cases} 1 - p_i & , i = j \\ -\sqrt{p_i p_j} & , i \neq j \end{cases}. \quad (39)$$

The $i = j$ result is the well known one for a binomial distribution. The $i \neq j$ result is negative because particles in different bins are anti-correlated: more (less) particles in one bin leads to less (more) in other bins on average due to a fixed total number of particles.

As shown above there are nonstatistical fluctuations due to sources, Bose-Einstein fluctuations, resonances, etc., and — in particular — density fluctuations. As in Eq. (20) we assume that the multiplicity consist of particles from a HM and a QM phase. The covariances in Eq. (21) are derived analogously to Eq. (21)

$$\omega_{ij} = \omega_{ij,HM} + (\omega_{ij,QM} - \omega_{ij,HM}) \frac{\langle N_{i,QM} \rangle}{\langle N_i \rangle}, \quad (40)$$

when $\langle N_i \rangle = \langle N_j \rangle$; when different the general formula is a little more complicated. Now, the hadronic fluctuations $\omega_{ij,HM}$ is of order unity for $i = j$, smaller for adjacent bins and vanishes or even becomes slightly negative according to (39) for bins very different in pseudorapidity or azimuthal angle ϕ . The QM fluctuations are much larger: $\omega_{i,QM} \sim \langle N_{i,QM} \rangle$ (see the discussion after Eq. (19)). In order to discriminate the QM fluctuations from the hadronic ones, Eq. (40) requires

$$\langle N_{i,QM} \rangle \gtrsim \sqrt{(\omega_{ij} - \omega_{ij,HM}) \langle N_i \rangle}. \quad (41)$$

If we assume $N_{Tot} \sim 8000$ and group the BRAHMS detector segments into 8 along the beamline, $\langle N_i \rangle \sim 1000$. To see a clear increase in fluctuations, say $\Delta\omega \equiv \omega_{ij} - \omega_{ij,HM} \sim 1$, a density fluctuation of only $\langle N_{i,QM} \rangle \gtrsim \sqrt{N_i} \sim 30$ particles are required corresponding to a few percent of the average. By analysing many events (of the same total multiplicity) the accuracy by which fluctuations are measured experimentally is greatly improved. Generally, $\Delta\omega \sim 1/\sqrt{N_{events}}$, and so fluctuations can in principle be determined with immense accuracy.

It may be advantageous to correlate bins with the same pseudorapidity but different azimuthal angles since the hadronic correlations between these are small whereas QM fluctuations remain.

7 HBT

Particle interferometry was invented by Hanbury-Brown & Twiss (HBT) for stellar size determination [1] and is now employed in nuclear collisions [1,10,45]. It is a very powerful method to determine the 3-dimensional source sizes, lifetimes, duration of emission, flow, etc. of pions, kaons, etc. at freeze-out. Since the number of pairs grow with the multiplicity per event squared the HBT method will become even better at RHIC and LHC colliders where the multiplicity will be even higher.

The use of HBT to extract the system geometry is a familiar application of

event-by-event fluctuations in nuclear collisions [1]. We shall here describe how HBT in combination with density fluctuations can be exploited to reveal the size of the sources for fluctuations as well as being a complementary signal [46].

7.1 The correlation function

The standard HBT method for calculating the Bose-Einstein correlation function from the interference of two identical particles is now briefly discussed. For a source of size R we consider two particles emitted a distance $\sim R$ apart with relative momentum $\mathbf{q} = (\mathbf{k}_1 - \mathbf{k}_2)$ and average momentum, $\mathbf{K} = (\mathbf{k}_1 + \mathbf{k}_2)/2$. Typical heavy ion sources in nuclear collisions are of size $R \sim 5$ fm, so that interference occurs predominantly when $q \lesssim \hbar/R \sim 40$ MeV/c. Since typical particle momenta are $k_i \gtrsim K \sim 300$ MeV/c, the interfering particles travel almost parallel, i.e., $k_1 \simeq k_2 \simeq K \gg q$. The correlation function due to Bose-Einstein interference of identical spin zero bosons as $\pi^\pm \pi^\pm$, $K^\pm K^\pm$, etc. from an incoherent source is [1]

$$C_2(\mathbf{q}, \mathbf{K}) = 1 \pm \left| \frac{\int d^4x S(x, \mathbf{K}) e^{iqx}}{\int d^4x S(x, \mathbf{K})} \right|^2, \quad (42)$$

where $S(x, \mathbf{K})$ is the source distribution function describing the phase space density of the emitting source.

Experimentally the correlation functions are often parametrized by the gaussian form

$$C_2(q_s, q_o, q_l) = 1 + \lambda \exp[-q_s^2 R_s^2 - q_o^2 R_o^2 - q_l^2 R_l^2 - 2q_o q_s R_{os}^2 - 2q_o q_l R_{ol}^2]. \quad (43)$$

Here, $\mathbf{q} = \mathbf{k}_1 - \mathbf{k}_2 = (q_s, q_o, q_l)$ is the relative momentum between the two particles and $R_i, i = s, o, l, os, ol$ the corresponding sideward, outward, longitudinal, out-sideward and out-long HBT radii respectively. We have suppressed the \mathbf{K} dependence. We will employ the standard geometry, where the *longitudinal* direction is along the beam axis, the *outward* direction is along \mathbf{K}_t , and the *sideward* axis is perpendicular to these. Usually, each pair of particles is lorentz boosted longitudinal to the system where their rapidity vanishes, $y = 0$. Their average momentum \mathbf{K} is then perpendicular to the beam axis and is chosen as the outward direction. In this system the pair velocity $\boldsymbol{\beta}_{\mathbf{K}=\mathbf{K}} = \mathbf{K}/E_K$ points in the outward direction with $\beta_o = p_t/m_\perp$, where $m_\perp = \sqrt{m^2 + p_\perp^2}$ is the transverse mass, and the out-longitudinal coupling R_{ol} vanish at midrapidity [49]. Also R_{os} vanishes for a cylindrically symmetric source or if the azimuthal angle of the reaction plane is not determined and therefore averaged over — as has

been the case experimentally so far. The reduction factor λ in Eq. (43) may be due to long lived resonances [48,37], coherence effects, incorrect Coulomb corrections or other effects. It is $\lambda \sim 0.5$ for pions and $\lambda \sim 0.9$ for kaons.

7.2 HBT for droplets

Droplets lead to spatial fluctuations in density which can be probed by correlations between identical particles [1]. For simplicity we parametrize these droplets by spatial and temporal gaussians of size R_d and duration of emission t_d . The distribution of particles in space and time — usually referred to as the source — for droplets situated at $x_i = (\mathbf{r}_i, t_i)$ is

$$S(x, K) \sim \sum_i \tilde{S}(x_i, K) \exp \left[-\frac{(\mathbf{r} - \mathbf{r}_i)^2}{2R_d^2} - \frac{(t - t_i)^2}{2t_d^2} \right], \quad (44)$$

where $\tilde{S}(x_i, K)$ is the distribution of sources. Normalizations of S cancel when calculating correlation functions, Eq.(42). Other effects as transverse flow, opacities [50], resonances [37], etc. can be included but we shall ignore them here for simplicity. Likewise, the extension to droplets of different size and duration of emission is straight forward but unnecessary for our purpose. We expect the scale of \tilde{S} is the nuclear overlap size R_A of order several *fermi*'s whereas the droplet size R_d is smaller — of order a few *fermi*'s.

From (42) and (44) we obtain

$$C_2(q) \simeq 1 + \exp[-\mathbf{q}^2 R_d^2 - (\mathbf{q} \cdot \beta)^2 t_d^2] |\tilde{S}(q, K)|^2, \quad (45)$$

where

$$\tilde{S}(q, K) = \sum_i \tilde{S}(x_i, K) e^{iq \cdot x_i} / \sum_i \tilde{S}(x_i, K) \quad (46)$$

is the Fourier transform of the distribution of sources and $\beta = \mathbf{K}/K_0$ is the average velocity of the pair.

If there is only a single droplet $\tilde{S}(q, K) = 1$ and the correlation function is simply given by the droplet gaussian. If there are many droplets, the sum can be replaced by an integral.

For non-expanding sources we can assume that the particle momentum distribution is the same for all droplets, i.e., independent of \mathbf{K} .

For many droplets we assume that the droplets are distributed by a gaussian

$$\tilde{S}(x_i, K) \sim \exp(-\mathbf{r}_i^2/2R_A^2 - t_i^2/2R_A^2), \quad (47)$$

where t_A is the spread in droplet formation times and R_A is the size of the nuclear overlap zone. It increases with decreasing impact parameter - roughly as $R_A(b) \simeq \sqrt{R_A(0)^2 - b^2}$, where $R_A(0) \simeq 1.2A^{1/3}fm$ is the nuclear size.

The resulting correlation function becomes

$$C_2(q) \simeq 1 + \exp[-\mathbf{q}^2(R_A^2 + R_d^2) - (\mathbf{q} \cdot \beta)^2(t_A^2 + t_d^2)]. \quad (48)$$

Since R_A and ct_A are typically of nuclear scales $\sim 5 - 10$ fm whereas we expect $R_d \sim 1$ fm, the droplets are simply “drowned” in the background of the other droplets.

In the case of only two droplets (of same size) the resulting correlation function is

$$C_2(q) \simeq 1 + \exp[-\mathbf{q}^2 R_d^2 - (\mathbf{q} \cdot \beta)^2 t_d^2] \cos\left(\frac{1}{2}q \cdot (x_1 - x_2)\right). \quad (49)$$

However, as the x_i 's differ from event to event the oscillation in (49) will, when summing over events, result in a Fourier transform over the distribution of x_i 's in different event and the end result will be similar to (48). The number of pairs in a single event at RHIC energies is probably not large enough to do event-by-event HBT. The oscillation will also be smeared by resonances, Coulomb effects, a hadronic background, etc.

We conclude that it will be very difficult to see the individual droplets through HBT when the sources do not expand.

At RHIC energies the collision regions are rapidly expanding particularly in the longitudinal direction. Consequently the droplets may have different expansion velocities and rapidities and the distribution $\tilde{S}(x_i, K)$ will depend on K and this difference will now be exploited.

When the droplets are separated in rapidity such that $|\eta_i - \eta_j| \gtrsim \sqrt{T/m_\perp}$, only particles within the same droplet contribute to the correlation function. If we transform to the droplet center-of-mass system, i.e. $\eta_i = 0$, the correlation function is then given by (48) with $\tilde{S} = 1$. In terms of q_s, q_o, q_l it can be written

$$C_2(q) = 1 + \exp \left[-q_s^2 R_d^2 - q_o^2 (R_d^2 + \beta_o^2 t_d^2) - q_l^2 (R_d^2 + \beta_l^2 t_d^2) - 2q_o q_l \beta_o \beta_l t_d^2 \right], \quad (50)$$

where $\beta_o = p_\perp/m_\perp \cosh(Y)$ and $\beta_l = \tanh(Y)$, are the transverse (outward) and longitudinal velocities respectively of the pair.

When the droplets overlap in rapidity, we need to consider the distribution of droplets in more detail. At ultrarelativistic energies the rapidity distribution is expected to display approximate Bjorken scaling, i.e., the rapidity distribution

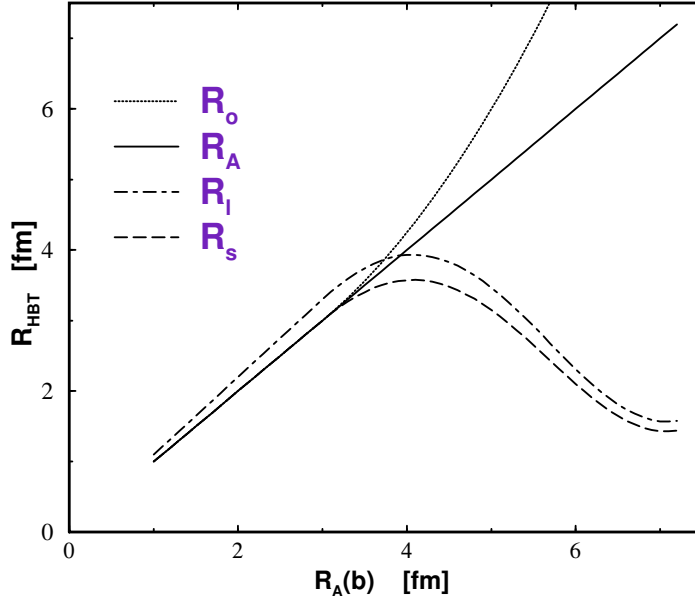


Fig. 13. The HBT radii as function of nuclear overlap R_A which is proportional to centrality, dN/dy or E_\perp . Droplet formation is assumed to set from semicentral collisions. A long mixed phase will then lead to large outward HBT radius R_o whereas triggering on large rapidity fluctuations corresponding to small droplets leads to smaller longitudinal R_l and sideward R_s HBT radii.

is approximately given by (2) where the droplet rapidities η_i are more or less evenly distributed between target and projectile rapidities. Parametrizing the transverse and temporal distribution as gaussians, we arrive at the droplet distribution

$$\tilde{S}(x_i, K) \sim \exp \left[-\frac{m_\perp}{T} \cosh(Y - \eta_i) - \frac{\mathbf{r}_{\perp,i}^2}{2R_A^2} - \frac{(\tau_i - \tau_f)^2}{2t_A^2} \right], \quad (51)$$

where $\tau_i = \sqrt{t_i^2 - z_i^2}$ is the invariant time and τ_f the average freeze-out time.

The resulting correlation function becomes (in the system $Y = 0$, where $\beta_l = \tanh Y = 0$ and $\beta_o = p_\perp/m_\perp$)

$$C_2(q) = 1 + \exp \left[-q_s^2(R_A^2 + R_d^2) - q_o^2(R_A^2 + R_d^2 + \beta_o^2(t_A^2 + t_d^2)) - q_l^2 \left(\tau_f^2 \frac{T}{m_\perp} + R_d^2 \right) \right]. \quad (52)$$

We observe that the larger nuclear size R_A dominates the smaller droplet size R_d when droplets overlap.

7.3 Centrality dependence of HBT radii

We can now study the consequences of forming droplets at RHIC energies. The onset of large rapidity fluctuations is one signal but it should be accompanied by the following behavior of the HBT radii. In peripheral collisions, where the nuclear overlap and stopping is small, we do not expect sufficient energy densities to build up and form droplets. Thus the HBT radii should simply grow with the size of the geometrical nuclear overlap, centrality, dN/dy and transverse energy E_T . At SPS energies the HBT radii are indeed found to scale approximately with the geometrical sizes of the colliding systems as given by (52).

If energy densities achieved in RHIC collisions are sufficient to form droplets in central collisions, the HBT radii will deviate from the geometrical overlap if triggered on large rapidity fluctuations (see Fig. 13) as given by Eq.(50). Comparing the theoretical predictions of Eqs. (50) and (52) with the experimentally measured HBT radii of Eq.(43) we see that the sideward and longitudinal HBT radii decrease from the nuclear size R_A, t_A to the droplet sizes R_d, t_d . Thus at a certain semi-centrality, where energy densities achieved in nuclear collisions start becoming large enough to create droplets, the sideward and longitudinal HBT radii should bend over and start decreasing with centrality. The outward HBT radius may behave differently depending on the duration of emission. The droplets may emit hadrons for a long time, as is the case for a long lived mixed phase (referred to as the “burning log”). In the hydrodynamic calculation of Ref. [51]), the duration of emission and consequently the outward HBT radius increase drastically up to five times larger than the transverse size of the system, i.e. R_A . This scenario is indicated in Fig. 13.

Besides droplets we may expect some hadronic background. It is straight forward to include such one in the correlation function. As its spatial extend is expected to be on the scale $\sim R_A$, it will reduce the correlation function at small $q \sim \hbar/R_A$. However, the droplets will still lead to correlations at large relative momenta of order $q \sim \hbar/R_d$. The large q correlations are suppressed by the square of the fraction of pions emerging from droplets at a given rapidity.

8 Summary

If first order transitions occur in high energy nuclear collisions, density fluctuations are expected which may show up in rapidity and multiplicity fluctuations event-by-event. The fluctuation can be enhanced by several orders of magnitude in case of droplet formation as compared to that from an or-

dinary hadronic scenario. Likewise a number of other observables as charged and neutral pions, kaons, photons, J/Ψ , etc., and their ratios can show anomalous correlations and enhancement or suppression of fluctuations as discussed above. This clearly demonstrates the importance of event-by-event fluctuations accompanying phase transitions, and illustrates how monitoring such fluctuations versus centrality becomes a promising signal, in the upcoming RHIC experiments, for the onset of a transition. The potential for enhanced or suppressed fluctuations (orders of magnitude) from a transition makes it worth looking for at RHIC considering the relative simplicity and accuracy of multiplicity fluctuation measurements.

An analysis of fluctuations in central Pb+Pb collisions as currently measured in NA49 do, however, not show any sign of anomalous fluctuations. Fluctuations in multiplicity, transverse momentum, K/π and other ratios can be explained by standard statistical fluctuation and additional impact parameter fluctuations, acceptance cuts, resonances, thermal fluctuations, etc. This understanding by “standard” physics should be taken as a baseline for future studies at RHIC and LHC and searches for anomalous fluctuations and correlations from phase transitions that may show up a number of observables.

By varying the acceptance one should be able to determine quantitatively the amount of thermalization in relativistic heavy ion collisions as function of centrality. In the thermal limit the fluctuations are independent of the acceptance and given by Eq. (16). In the opposite limit of few rescatterings among produced particles, the participant nucleon model gives acceptance dependent fluctuations, Eq. (10), and the ratio of Eq. (18) then gives the degree of thermalization. For peripheral collisions, where only few rescatterings occur, we expect the WNM to be approximately valid and the degree of thermalization to be small. For central collisions, where many rescatterings occur among produced particles, we expect to approach the thermal limit and the degree of thermalization should be close to 100%.

HBT interferometry adds an important space-time picture to the purely momentum space information one gets from single particle spectra. Triggering on rapidity fluctuations, the HBT radii may display a curious behavior. The outward HBT radius R_o may increase drastically with centrality due to a long lived mixed phase. The longitudinal R_l and sideward R_s HBT radii will, however, saturate and *decrease* for the very central collisions because a large rapidity fluctuation signals a hot and dense droplet of small size. The predicted behavior for the sideward and longitudinal HBT radii is *opposite* to that predicted in cascade and hydrodynamic calculations. It would be a clean signal of a first order phase transition in nuclear collisions.

Acknowledgement

I am much grateful to my collaborators G. Baym and A.D. Jackson on some of the work described in this report. Discussion with NA44 and Brahms (J.J. Gårdhøje, C. Holm, et al.), WA98 (T. Nayak), NA49 (G. Roland), J. Bondorf, S. Jeon, V. Koch, are gratefully acknowledged.

9 Appendix A

As fluctuations for a source model appears again and again (see Eqs. 8,10,17,21) we shall derive this simple equation in detail.

We define the fluctuations for any stochastic variable x as

$$\omega_x = \frac{\langle x^2 \rangle - \langle x \rangle^2}{\langle x \rangle}. \quad (53)$$

It is usually of order unity and therefore more convenient than variances. For a Poisson distribution, $P_N = e^{-\alpha} \alpha^N / N!$, the fluctuation is $\omega_N = 1$. For a binomial distribution with tossing probability p the fluctuation is $\omega_N = 1 - p$, independent of the number of tosses. In heavy ion collisions several processes add to fluctuations so that typically $\omega_N^{exp} \sim 1 - 2$.

Generally, when the multiplicity (N) arise from independent sources (N_p) such as participants, resonances, droplets or whatever,

$$N = \sum_{i=1}^{i=N_p} n_i, \quad (54)$$

where n_i is the number of particles produced in source i . In the absence of correlations between N_p and n , the average multiplicity is $\langle N \rangle = \langle N_p \rangle \langle n \rangle$. Here, $\langle \dots \rangle$ refer to averaging over each individual (independent) source as well as the number of sources. The number of sources vary from event to event and average is performed over typically $N_{events} \sim 100.000$ events as in NA49 or $N_{events} \sim 10^6$ in WA98.

Squaring Eq. (54) assuming that the source emit particles independently, i.e. $\langle n_i n_j \rangle = \langle n_i \rangle \langle n_j \rangle$ for $i \neq j$, the square consists of the diagonal and off-diagonal elements:

$$\langle N^2 \rangle = \langle N_p \rangle \langle n_i^2 \rangle + \langle N_p(N_p - 1) \rangle \langle n_i \rangle. \quad (55)$$

With (53) we obtain the multiplicity fluctuations

$$\omega_N = \frac{\langle N^2 \rangle - \langle N \rangle^2}{\langle N \rangle} = \omega_n + \langle n \rangle \omega_{N_p},$$

as in Eq. (8).

References

- [1] R. Hanbury–Brown and R.Q. Twiss, *Phil. Mag.* **45** (1954) 633. U. Heinz and B.V. Jacak, *Ann. Rev. Nucl. Part. Sci.* **49** (1999), and references therein.
- [2] S. Trentalange and S.U. Pandey, *J. Acoust. Sci. Am.* **99**, 2439 (1996); C. Slotta and U. Heinz, *Phys. Rev. D* **58**, 526 (1998).
- [3] M.R. Andrews, C.G. Townsend, H.-J. Miesner, D.S. Durfee, D. M. Kurn, and W. Ketterle, *Science* **275**, 637 (1997); Y. Castin and J. Dalibard, *Phys. Rev. A* **55**, 4330 (1997); G. Baym, A.J. Leggett, and C.J. Pethick, to be published.
- [4] See, e.g., J. Phillips et al., *astro-ph/0001089*.
- [5] M. Toscano et al., *Mon. Not. R. Astron. Soc.*, *astro-ph/9811398*.
- [6] G. Baym, G. Friedman, and I. Sarcevic, *Phys. Lett.* **219B**, 205 (1989).
- [7] H. Heiselberg, G.A. Baym, B. Blättel, L.L. Frankfurt, and M. Strikman, *Phys. Rev. Lett.* **67**, 2946 (1991); B. Blättel, G.A. Baym, L.L. Frankfurt, H. Heiselberg and M. Strikman, *Nucl. Phys.* **A544**, 479c (1992).
- [8] G. Baym, B. Blättel, L. L. Frankfurt, H. Heiselberg, and M. Strikman, *Phys. Rev. C* **52**, 1604 (1995).
- [9] T. Åkesson et al. (Helios collaboration), *Z. Phys.* **C38**, 383 (1988).
- [10] G. Roland et al., (NA49 collaboration), *Nucl. Phys.* **A638**, 91c (1998); H. Appelhäuser et al., (NA49 collaboration), *Phys. Lett.* **B459** (1999) 679.
- [11] M. Gaździcki and S. Mrówczyński, *Z. Phys.* **C54** 127 (1992).
- [12] S. Mrówczyński, *Phys. Rev. C* **57**, 1518 (1998); *Phys. Lett.* **B430**, 9; *ibid.* **B439**, 6 (1998); *ibid.* **B465**, 8 (1999); and *nucl-th/9907099*.
- [13] M. Stephanov, K. Rajagopal, and E. Shuryak, *Phys. Rev. Lett.* **81**, 4816 (1998); K. Rajagopal, *hep-th/9808348*; B. Berdnikov and K. Rajagopal, *Phys. Rev. D.* **61**, 105017 (2000).
- [14] S. Gavin and C. Pruneau, *nucl-th/9906060*; *nucl-th/9907040*; S. Gavin, *nucl-th/9908070*.
- [15] S.A. Voloshin, V. Koch, H.G. Ritter, *nucl-th/9903060*.

- [16] G. Baym and H. Heiselberg, *Phys. Lett.* **B469** (1999) 7.
- [17] C. Bernard et al., *Phys.Rev.* **D55** (1997) 6861; Y. Iwasaki, K. Kanaya, S. Kaya, S. Sakai, T. Yoshi, *Phys. Rev. D* **54**, 7010 (1996).
- [18] G. Boyd et al, *Phys. Rev. Lett.* 75 (1995) 4169. E. Laermann, Proc. *Quark Matter '96*, Nucl. Phys. A610 (1996) 1c.
- [19] K. Eskola, hep-ph/9911350.
- [20] L.D. Landau & E.M. Lifshitz, *Statistical Physics, Part 1* (Pergamon, 1980).
- [21] J.I. Kapusta, A.P. Vischer, *Phys. Rev.* **C52** (1995) 2725. E.E. Zabrodin, L.P. Csernai, J.I. Kapusta, G. Kluge, *Nucl. Phys.* **A566** (1994) 407c.
- [22] M.A. Halasz, A.D. Jackson, R.E. Shrock, M.A. Stephanov, J.J.M. Verbaarschot, *Phys. Rev. D* **58**, 96007 (1998)
- [23] J. Bjorken, *Phys. Rev.* **D27** (1983) 140; M. Alford, K. Rajagopal and F. Wilczek, *Phys. Lett.* **B422** (1998) 247; and nucl-th/9903502.
- [24] A. Bialas, M. Bleszynski and W. Czyz, *Nucl. Phys.* **B111** (1976) 461.
- [25] J. Whitmore, *Phys. Rep.* **27**, 187 (1976).
- [26] H. Bøggild and T. Ferbel, *Ann.Rev.Nucl. Sci.* **24**, 451 (1974)
- [27] UA5 Collaboration, G. J. Alner et al., *Phys. Rep.* **154**, 247 (1987).
- [28] E735 Collaboration, C. S. Lindsey et al., *Nucl. Phys. A* **544**, 343c (1992);
- [29] Z. Koba, H. B. Nielsen and P. Olesen, *Nucl. Phys.* **B40**, 317 (1972).
- [30] S. Voloshin (NA49), private comm.
- [31] K. Werner, private communication.
- [32] M. Gazdzicki & O. Hansen, *Nucl. Phys.* **A528** (1991) 754; W. Wroblewski, *Acta Phys. Pol.* **B4** (1973) 857.
- [33] H. Heiselberg and A. Levy, *Phys. Rev.* **C59** (1999) 2716.
- [34] J. Schukraft et al. (NA34 collaboration), *Nucl. Phys.* **A498**, 79c (1989).
- [35] T.K. Nayak (WA98 collaboration), private communication.
- [36] G. Bertsch, *Phys. Rev. Lett.* **72**, 2349 (1994).
- [37] H. Heiselberg, *Phys. Lett.* **B379** (1996) 27. U.A. Wiedemann and U. Heinz, *Phys. Rev.* **C56** (1997) 3265.
- [38] S. Jeon and V. Koch, *Phys.Rev.Lett.* **83** (1999) 5435
- [39] NA50 Collaboration, M.C. Abreu et al., *Phys. Lett.* **B410**, 327 (1997); *ibid* 337; CERN-EP/99-13, to appear in *Phys. Lett. B*.
- [40] T. Matsui and H. Satz, *Phys. Lett.* 178B, 416 (1991)

- [41] H. Heiselberg and R. Mattiello, *Phys. Rev. C* **60** (1999) 44902
- [42] I.G. Bearden et al. (NA44 collaboration), *Phys. Rev. Lett.* **78** (1997) 2080.
- [43] J.G. Reid et al., NA49 collaboration, QM99.
- [44] J.J. Gaardhøje, BRAHMS collaboration, priv. comm.
- [45] A. Franz, *Nucl. Phys. A* **610** (1996) 240c. I.G. Bearden et al., *Phys. Rev.* **C58** (1998) 1656.
- [46] H. Heiselberg and A.D. Jackson, *Proc. Adv. in QCD*, Minnesota, May 1998, *nucl-th/9809013*.
- [47] M. Gyulassy, D. H. Rischke, B. Zhang *Nucl.Phys. A* **613**, 397 (1998).
- [48] T. Csörgő and B. Lörstad, *Nucl. Phys.* **A590**, 465c (1995); *Phys. Rev.* **C54** (1996) 1390.
- [49] S. Chapman, J.R. Nix, and U. Heinz, *Phys. Rev.* **C52**, 2694 (1995).
- [50] H. Heiselberg, *Phys. Rev. Lett.* **82** (1999) 2052.
- [51] S. Bernard, D.H. Rischke, J.A. Maruhn, W. Greiner *Nucl. Phys.* **A625**, 473 (1997).